



Deposited via The University of York.

White Rose Research Online URL for this paper:

<https://eprints.whiterose.ac.uk/id/eprint/169736/>

Version: Accepted Version

Article:

Barrett, James, Girr, Philipp and Mackinder, Luke (2021) Pyrenoids: CO₂-fixing phase separated liquid organelles. *Biochimica et biophysica acta-Molecular cell research*. 118949. ISSN: 0167-4889

<https://doi.org/10.1016/j.bbamcr.2021.118949>

Reuse

This article is distributed under the terms of the Creative Commons Attribution-NonCommercial-NoDerivs (CC BY-NC-ND) licence. This licence only allows you to download this work and share it with others as long as you credit the authors, but you can't change the article in any way or use it commercially. More information and the full terms of the licence here: <https://creativecommons.org/licenses/>

Takedown

If you consider content in White Rose Research Online to be in breach of UK law, please notify us by emailing eprints@whiterose.ac.uk including the URL of the record and the reason for the withdrawal request.

1 **Pyrenoids: CO₂-fixing phase separated liquid organelles**

2
3 James Barrett^{1*}, Philipp Girr^{1*}, Luke C.M. Mackinder¹

4
5 ¹Department of Biology, University of York, York, YO10 5DD, UK

6 *Equal contribution

7 8 **ABSTRACT**

9
10 Pyrenoids are non-membrane bound organelles found in chloroplasts of algae and hornwort
11 plants that can be seen by light-microscopy. Pyrenoids are formed by liquid-liquid phase
12 separation (LLPS) of Rubisco, the primary CO₂ fixing enzyme, with an intrinsically disordered
13 multivalent Rubisco-binding protein. Pyrenoids are the heart of algal and hornwort biophysical
14 CO₂ concentrating mechanisms, which accelerate photosynthesis and mediate about 30% of
15 global carbon fixation. Even though LLPS may underlie the apparent convergent evolution of
16 pyrenoids, our current molecular understanding of pyrenoid formation comes from a single
17 example, the model alga *Chlamydomonas reinhardtii*. In this review, we summarise current
18 knowledge about pyrenoid assembly, regulation and structural organization in
19 *Chlamydomonas* and highlight evidence that LLPS is the general principle underlying pyrenoid
20 formation across algal lineages and hornworts. Detailed understanding of the principles behind
21 pyrenoid assembly, regulation and structural organization within diverse lineages will provide
22 a fundamental understanding of this biogeochemically important organelle and help guide
23 ongoing efforts to engineer pyrenoids into crops to increase photosynthetic performance and
24 yields.

25 26 **INTRODUCTION**

27 28 **CO₂ concentrating mechanisms accelerate photosynthesis**

29 Photosynthesis is the gateway between inorganic carbon (i.e. CO₂) and organic carbon in the
30 global carbon cycle. It harnesses energy from sunlight to annually reduce ~400 gigatonnes of
31 CO₂ (Net Primary Production; [1]) whilst simultaneously releasing O₂. Given that nearly all
32 carbon fixation is performed by Ribulose-1,5-bisphosphate carboxylase oxygenase (Rubisco),
33 it is puzzling that over its >3.5 billion year existence it has remained slow (catalytic rates
34 typically 8-10 times lower than the median for central metabolic enzymes [2]) and has a
35 relatively poor selectivity for CO₂ over O₂ under current atmospheric concentrations of 0.04%
36 CO₂ and 21% O₂ [3]. These apparent limitations appear to be due to a trade-off between
37 Rubisco's catalytic rate and its specificity for CO₂ over O₂ [4-6], with oxygenation resulting in
38 energetically wasteful photorespiration. To overcome Rubisco's "bottle-neck" photosynthetic
39 organisms have evolved diverse strategies. Many terrestrial plants attain high CO₂ fixation and
40 reduce photorespiration by investing large amounts of resources into Rubisco that is
41 catalytically slow but has a relatively high CO₂/O₂ specificity. This results in Rubisco typically
42 accounting for approximately 25% of soluble protein in plant leaves [7], making it potentially
43 the most abundant enzyme on earth [8, 9]. An alternative strategy evolved by some plants and
44 nearly all aquatic photosynthetic organisms is to operate CO₂ concentrating mechanisms
45 (CCMs) that actively concentrate CO₂ at Rubisco's active site, thus enabling high CO₂ fixation
46 rates with lower amounts of faster, less specific Rubisco.

47 CCMs can be broadly split into two types: biochemical and biophysical. This review
48 focuses on biophysical CCMs, the dominant CCM type found in aquatic photosynthetic
49 organisms. Biophysical CCMs typically function via the concentration of inorganic carbon in
50 the form of bicarbonate (HCO_3^-) and its subsequent dehydration to CO_2 in a Rubisco rich
51 compartment. This functionality is achieved through out-of-equilibrium carbonate chemistry,
52 pH changes across membranes and the heterogeneous distribution of carbonic anhydrases
53 [10-13]. The slow, uncatalyzed equilibrium of HCO_3^- and CO_2 enables the accumulation of
54 HCO_3^- that has a lower membrane permeability as compared to uncharged species like CO_2 ;
55 pH determines the $\text{HCO}_3^-:\text{CO}_2$ ratio, with HCO_3^- ~100 times more abundant than CO_2 at pH 8,
56 thus enabling HCO_3^- concentration at higher pH or CO_2 release at lower pH; and the specific
57 spatial distribution of carbonic anhydrases enables the rapid equilibrium of HCO_3^- and CO_2 to
58 drive HCO_3^- formation for concentration or CO_2 release for Rubisco fixation.

59 Biophysical CCMs found in oxygenic phototrophs can be generally split into two types:
60 carboxysome based CCMs found in prokaryotic cyanobacteria, and pyrenoid based CCMs
61 found in eukaryotic algae and some non-vascular plants (i.e. most hornwort species).
62 Cyanobacterial carboxysomes are icosahedral 100+ megadalton protein assemblies where
63 densely aggregated Rubisco is encapsulated in a protein shell with a typical diameter of 150-
64 200 nm [14]. HCO_3^- concentrated in the cyanobacterial cytosol diffuses into the carboxysome
65 through hexameric shell proteins where it is dehydrated to CO_2 via carbonic anhydrase for
66 fixation by Rubisco. Algal pyrenoids are also Rubisco assemblies, but they are much larger
67 than carboxysomes (~1-2 μm diameter), are dynamic in size by growing and shrinking in
68 response to CO_2 and light, lack a proteinaceous shell, and are typically traversed by
69 membranes that are continuous with the thylakoid network [15]. These characteristic
70 membrane traversions are thought to be the primary source of inorganic carbon delivery,
71 where HCO_3^- is converted to CO_2 in the acidic lumen, creating a “point source” of CO_2 within
72 the pyrenoid.

73 Understanding CCMs at the molecular level across diverse species is critical for
74 understanding biotic contributions to the global carbon cycle and for providing engineering
75 solutions to address human driven pressures on our planet. CCM driven cyanobacterial and
76 algal photosynthesis accounts for approximately half of global net primary production [1] and
77 plays a critical role in the buffering of anthropogenic CO_2 -driven global warming through driving
78 the “biological pump” that moves carbon from the upper ocean to the deep ocean for long-term
79 storage [16]. In addition, modelling suggests that engineering crops with CCMs may
80 significantly increase photosynthetic performance. If these improvements translate to yield the
81 engineering of a CCM into crops such as rice, wheat and soya could increase yields by up to
82 60% [17], a significant step towards the goal of the predicted ~85% increases required to feed
83 the global population in 2050 [18].

84

85 **Box 1: General properties of LLPS systems**

86 Liquid-liquid phase separation (LLPS) is the process by which a homogeneous solution
87 reversibly demixes to form a dense phase that is distinguished from a coexisting dilute phase.
88 The solution composition, concentration and conditions (pH, temperature etc.) define a phase
89 diagram for demixing that is bounded by a coexistence line (also known as the binodal) that
90 determines the one- and two-phase states (Figure 1).

91
92

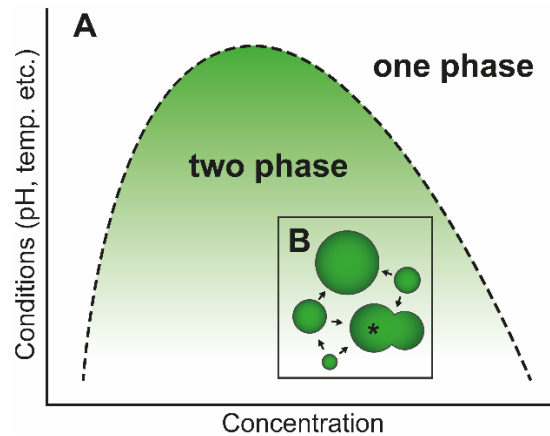


Figure 1. Phase diagrams explain LLPS. A) A phase diagram determines a one- and two-phase state of the system, where the two-phase state consists of droplets distinguished from the coexisting dilute phase. Changes in solution conditions that affect interaction strength (y) and concentration of components (x) alter the phase state of the system relative to the coexistence line (black dashed). **B)** Schematic of droplet growth where Ostwald ripening is shown with arrows that indicate the trafficking of solute from smaller to larger droplets. Asterisk indicates coalescence of two adjacent demixed droplets.

In biology, LLPS is thought to give rise to an array of membraneless bodies [19] that provide spatiotemporal control over diverse cellular processes [20], by concentrating particular protein and nucleic acid species relative to the bulk phase [21], whilst permitting a rapidly diffusing biochemical environment [22]. Although membraneless bodies were described as early as 1803 [23], their liquid-like properties were demonstrated much more recently. Brangwynne et al. [24] reported fusion, dripping, fission and internal/external rearrangement of spherical P granules over second timescales in 2009. These observations hold true for many biomolecular condensates, where growth can occur by Ostwald ripening (growth of larger droplets at the expense of smaller droplets to reduce surface tension energetic penalty; Figure 1B) and elastic ripening (transport of solute down a stiffness gradient) in addition to coalescence (Figure 1B, asterisk) [25, 26]. It should be highlighted that many systems have been classified as LLPS based on these qualitative descriptions, though other mechanisms of biomolecular condensate assembly are possible, and quantitative descriptors are required for their distinction [27].

Given their liquid-like nature, it is postulated that membraneless bodies can respond more rapidly to environmental cues than membrane-bound compartments [28], and as such are implicated in many transitory processes across a vast array of cellular contexts. Their composition is often accordingly vast [29], and accompanied by an array of underpinning interactions, including electrostatic, π - π , cation- π , hydrophobic associations and hydrogen bonds between subsumed components [30]. These interactions are often weak in nature and high in valency (number of binding sites on a binding partner) to facilitate formation of a network of interactions, required for phase separation [31]. This network forms homotypically, in simple coacervation, or between multiple protein species in complex coacervation [19]. Across these coacervation mechanisms, multivalency is provided by a range of associating sequence and structural features, comprising folded and/or unfolded domains, that can be loosely termed 'stickers'. Variegating these stickers, are regions of structure or sequence that are termed 'spacers' [32]. Although often not directly involved in coacervation interactions, spacer presence and composition has marked effects on condensate properties, dependent

131 on their solvation properties, but little effect on phase separation driving forces has been
132 demonstrated [33]. Changes in valency, concentration and affinity of stickers sharply
133 determines phase separation thresholds [21] and coacervate composition [34]. These changes
134 often occur rapidly, through sharp transitions that can be influenced by a host of cellular
135 factors, both globally (pH, temperature and ionic strength - see Dignon et al. [30] for review)
136 and targeted (including methylation, phosphorylation, acetylation, SUMOylation - see Owen
137 and Shewmaker [35]), that account for condensate transiency.

138
139 Despite experiencing rapid transitions in response to relatively minute changes, biomolecular
140 condensates can be stable throughout generational lifetimes (e.g. the *Chlamydomonas*
141 *reinhardtii* pyrenoid that is inherited and maintained through multiple cell division events [36]),
142 whilst retaining their liquid-like properties. Owing to their liquid nature, condensate morphology
143 can be reversibly deformed, by wetting (adherence to solid surfaces due to intermolecular
144 interactions) [24], disruption [37] or compositional effects [38], commonly observed in the
145 cellular environment. Surface tension underpins this behaviour [39], and is affected by
146 coacervate component interaction strength and valency [38]. A range of viscosity is also
147 observed across coacervates and their lifetimes, and has been implicated in their functionality
148 [40]. The maturation of condensates to more solid states has been proposed to occur *in vivo*
149 [22], mirroring the effect of gelation (transition towards a less dynamic structure underpinned
150 by interaction strength increase) that influences droplet dynamics *in vitro* [41]. The mechanistic
151 implications of these macroscopic properties are relatively unexplored [30, 31], but are likely
152 central to condensate activity regulation and physical resilience. Accordingly, microscopic
153 perturbations that alter macroscopic properties are functionally intertwined. The movement of
154 species within biomolecular condensates is influenced by both macroscopic and microscopic
155 properties. The porosity of the primary scaffold components that constitute condensates
156 determines the relative mobility of their subsumed components in a size-dependent manner
157 [22], referred to as the mesh-size, that is dependent on the extent of physical cross links [31].
158 Microscopically, the interaction of diffusing species with the biomolecular scaffold will also
159 influence their mobility.

160 161 162 **Pyrenoid and carboxysome assembly is driven by disordered, multivalent Rubisco** 163 **binding proteins**

164 In recent years, it has become clear that aggregation of Rubisco by disordered, multivalent
165 binding proteins is a required precursor for formation of pyrenoids in the model alga
166 *Chlamydomonas reinhardtii* (*Chlamydomonas* from here on) and carboxysomes in model
167 cyanobacteria and proteobacteria [36, 42-44]. There are two types of carboxysomes, α and β ,
168 that appear to have evolved independently. Nearly all of their components have counterparts
169 across the carboxysome types, including a “linker” that interacts multivalently with Rubisco,
170 enabling liquid-liquid phase separation (LLPS) through complex coacervation (see Box 1 for
171 an introduction to general properties of LLPS systems) [14]. In the α -carboxysome, CsoS2
172 multivalently binds Rubisco driving carboxysome assembly whilst in the β -carboxysome CcmM
173 performs an analogous role. In both cases deletion of CsoS2 or CcmM abrogates
174 carboxysome assembly leading to a high-CO₂ requiring phenotype – the characteristic
175 signature of a non-functional CCM [45, 46]. Demixing occurs when truncated CsoS2 or CcmM,
176 containing only the multivalent Rubisco interacting domains, are mixed with the corresponding
177 Rubisco *in vitro* [43, 47]. It is postulated that Rubisco condensation may play a key role in

178 carboxysome assembly for both carboxysome types. However, the lack of Rubisco mobility
179 within β -carboxysomes suggests that the role of LLPS may be limited to assembly [48].

180 In contrast to the two evolutionary origins of carboxysomes, and the clear conservation of
181 carboxysome components across species [49], pyrenoid evolution appears to be far more
182 complex. Pyrenoids are thought to have evolved multiple times [15, 50] and there is apparent
183 absence of conserved structural components across diverse algal lineages (see Box 2 for an
184 overview of algal diversity) [15, 51]. Nearly all of our data on pyrenoid formation is based on
185 *Chlamydomonas*, where the multivalent disordered protein EPYC1 (Essential Pyrenoid
186 Component 1, formerly LCI5), causes the aggregation of Rubisco through complex
187 coacervation [36, 44, 51]. However, EPYC1 homologs are not found outside of closely related
188 green algae, making drawing conclusions of pyrenoid assembly across algal lineages difficult.
189 This review aims to integrate our current knowledge of the algal pyrenoid with the rapidly
190 advancing field of biological LLPS in a drive to identify key unanswered questions that can
191 guide our understanding of pyrenoid form and function across diverse algae to give insights
192 into this biogeochemically important organelle and help guide engineering efforts into crops to
193 increase yields.

194
195

196 **Box 2: Pyrenoid occurrence and overview of algal diversity**

197 Pyrenoids occur in all algal lineages and most hornworts (Figure 2) but are missing in all other
198 land plants (liverworts, mosses, and vascular plants). The high diversity of algae, their long
199 evolutionary history and pyrenoid apparent loss and reappearance means that pyrenoids
200 possibly have tens to hundreds of evolutionary origins [50]. Algae is a polyphyletic term for
201 mostly aquatic photosynthetic eukaryotes, which includes over 70,000 different extant species
202 [52]. The phylogeny of algae is controversial. For this review, we group algae into seven clades
203 according to their chloroplast ancestry [53]. The 1st clade, Archaeplastida, which contains
204 glaucophytes, rhodophytes (red algae) and green algae (core chlorophytes, charophytes and
205 prasinophytes) (and land plants), acquired their chloroplasts through a primary endosymbiosis
206 of a cyanobacterium. All other algal clades inherited their chloroplasts through secondary or
207 even tertiary endosymbiotic events. The 2nd clade, excavates, which contains only one
208 photosynthetic group (euglenids), and the 3rd clade, rhizaria, only containing photosynthetic
209 chlorarachniophytes, inherited their chloroplasts through a secondary endosymbiosis of a
210 green alga. The 4th clade, stramenopiles (containing xanthophytes, chrysophytes,
211 phaeophytes and bacilliarophytes/diatoms) inherited their chloroplasts through a secondary
212 endosymbiosis of a red alga. In the 5th clade, alveolates (containing dinoflagellates),
213 chloroplast inheritance is complex with species having secondary or tertiary plastids
214 originating from both red and green algal lineages. Algae belonging to clades 3, 4 and 5 are
215 often summarised to the TSAR supergroup (Figure 2). The 6th clade (containing haptophytes)
216 and the 7th clade (containing cryptophytes) both inherited their chloroplasts through a
217 secondary endosymbiosis of a red alga.

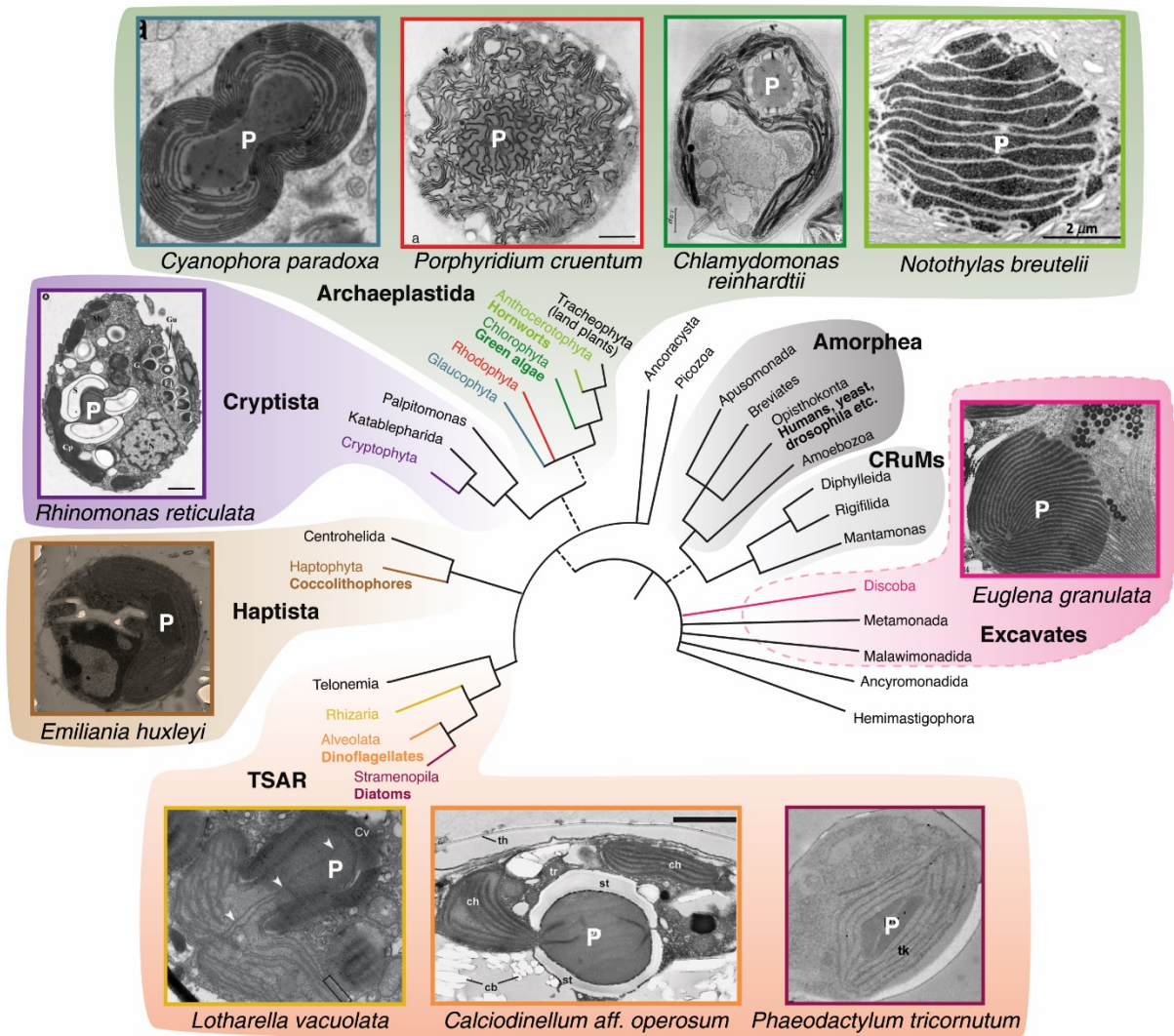
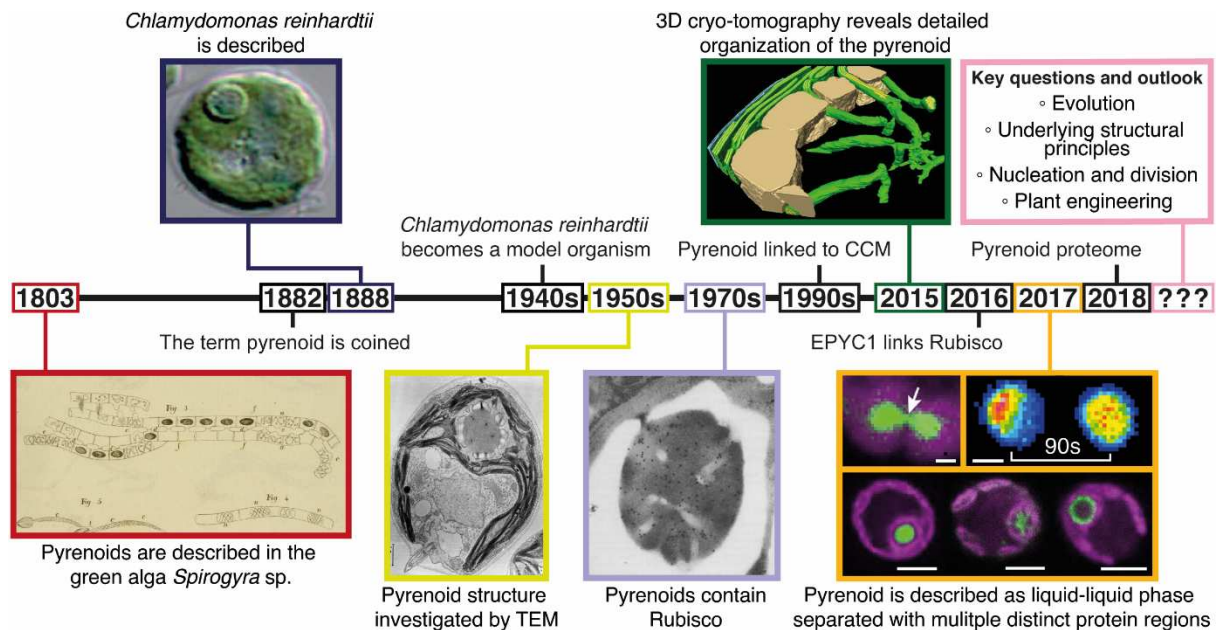


Figure 2. Pyrenoid containing algae are polyphyletic and found across the eukaryotic tree of life. Tree is based on Burki et al. [53]. Dashed lines indicate uncertainty about the monophyletic nature of these groups. Transmission electron microscope image descriptions (clockwise from top left): A dividing pyrenoid (also known as central body) of the glaucophyte *Cyanophora paradoxa* [54]. *Porphyridium cruentum* with thylakoid membranes stained dark via photooxidation of 3,3'-diaminobenzidine.4HCl (DAB) that depicts Photosystem I activity [55]. The model green alga *Chlamydomonas reinhardtii* [56]. *Notothylas breutellii* [57]. *Euglena granulata* [58]. The model diatom *Phaeodactylum tricornutum* [59]. The dinoflagellate *Calciadinellum aff. operosum* [60]. *Lotharella vacuolata* [61]. The abundant biogeochemically important calcifying coccolithophore *Emiliana huxleyi* (author's collection). *Rhinomonas reticulata* var. *atorrosea* [62]. P indicates pyrenoid.

A brief history of the pyrenoid

The relatively large size and high density of pyrenoids make them easy to see via light microscopy, with descriptions in algae referring to the pyrenoid from 1803 (Figure 3; [23]) and the first reports of pyrenoids in hornworts from 1885 [63]. As a result, pyrenoids may be the first LLPS organelles to be described, with the nucleolus described later in 1835 [64]. The term pyrenoid was coined in 1882 [65] and its presence and ultrastructural variation across

239 evolutionarily-diverse algae was described throughout the mid-1900s by the increased use of
 240 TEM imaging, which also allowed characterization of the pyrenoid ultrastructure. From early
 241 TEM images, it was assumed that the pyrenoid matrix, depending on the species, was either
 242 crystalline or amorphous. In the 1970s Rubisco was shown to be a major constituent by
 243 enzymatic characterization of purified pyrenoids and analysis of Rubisco knock-out lines [66-
 244 69], which was later confirmed by immunocytochemistry [70, 71]. The association between
 245 pyrenoid presence and efficient CCM function was first made in the 1990s, when experimental
 246 observations showed that pyrenoid containing algae have an efficient CCM, with CCM
 247 induction concurrent with biochemical and structural changes to the pyrenoid, whereas algae
 248 lacking a pyrenoid either lack a CCM or have a reduced ability to concentrate CO₂ [72-75].
 249 The discovery that EPYC1 linked Rubisco to form the pyrenoid was made in 2016 [51] and its
 250 LLPS nature identified in 2017 [36].
 251



252
 253
 254 **Figure 3. A brief history of the pyrenoid.** Pyrenoids were first described in the green alga
 255 *Spirogyra* by Jean-Pierre Vaucher in 1803. The original drawings by Vaucher display one
 256 ribbon-like chloroplast per cell that contains multiple spherical pyrenoids [23]. In 1882, the
 257 term pyrenoid (Greek *pyrene*, stone kernel-like) was coined by Friedrich Schmitz, who
 258 observed pyrenoids in several algae species [65]. Six years later, in 1888 the model alga
 259 *Chlamydomonas reinhardtii* was first described by Pierre Augustin Dangeard [76].
 260 *Chlamydomonas*, which is the central model for pyrenoid research, has one pyrenoid per
 261 cell that is visible in light microscopy (light microscopy image by Moritz Meyer [77]). In the
 262 1940s, *Chlamydomonas* entered into research labs and over time became an essential
 263 model system [78]. The use of TEM to image algae from the early 1950s onward made
 264 details of the pyrenoid ultrastructure with matrix, traversing thylakoids and starch sheath
 265 visible (TEM image of *Chlamydomonas* by Ohad et al. [56]). From the 1970s onward, it
 266 became clear that the pyrenoid contains most of the cell's Rubisco, which later in 1980s was
 267 incontrovertibly proved by immunogold labelling (TEM image of immunogold-labelled
 268 Rubisco (black dots) in *Chlamydomonas* by Lacoste-Royal et al. [70]). The first associations
 269 of the pyrenoid with the CCM were made in the 1990s. In 2015, the 3D structure of the
 270 *Chlamydomonas* pyrenoid was resolved by cryo-EM tomography (reconstruction of the
 271 pyrenoid (thylakoid tubules in green, starch sheath in beige, matrix is not displayed) by Engel
 272 et al. [79]). EPYC1 and its function as a Rubisco linker in the *Chlamydomonas* pyrenoid was

273 discovered in 2016 [51]. In 2017 it was shown that the pyrenoid is formed by liquid-liquid
274 phase separation (top left, the pyrenoid divides via fission; top right, fluorescent recovery
275 after photobleaching shows that Rubisco undergoes internal mixing over second timescales
276 in the pyrenoid) [36] and multiple distinct protein regions were described, including the
277 pyrenoid matrix (left, Rubisco), pyrenoid tubules (middle, PSAH) and starch sheath (right,
278 LCI9) [80] (fluorescence microscopy images (magenta: chlorophyll, green: labelled protein).
279 Zhan et al. [81] reported a pyrenoid proteome in 2018.
280

281 **STRUCTURE AND FUNCTION OF THE *CHLAMYDOMONAS* PYRENOID**

282

283 The functionality of pyrenoids to concentrate CO₂ at Rubisco's active site to enhance
284 carboxylation requires structural features in addition to the formation of the pyrenoid matrix
285 through Rubisco-EPYC1 condensation. Central to CO₂ concentration and pyrenoid function is
286 the shuttling of inorganic carbon through the subcellular environment to Rubisco within the
287 pyrenoid. The spatial segregation of a carbonic anhydrase within the pyrenoid is essential for
288 catalysing the subsequent dehydration of inorganic carbon (in the form of HCO₃⁻) to CO₂,
289 allowing release for carboxylation by Rubisco in the pyrenoid matrix. As discussed above,
290 these characteristics are considered basal for the function of biophysical CCMs and are thus
291 expected to be conserved across pyrenoid-based CCMs, despite ultrastructural variations
292 (Figures 2 and 6).

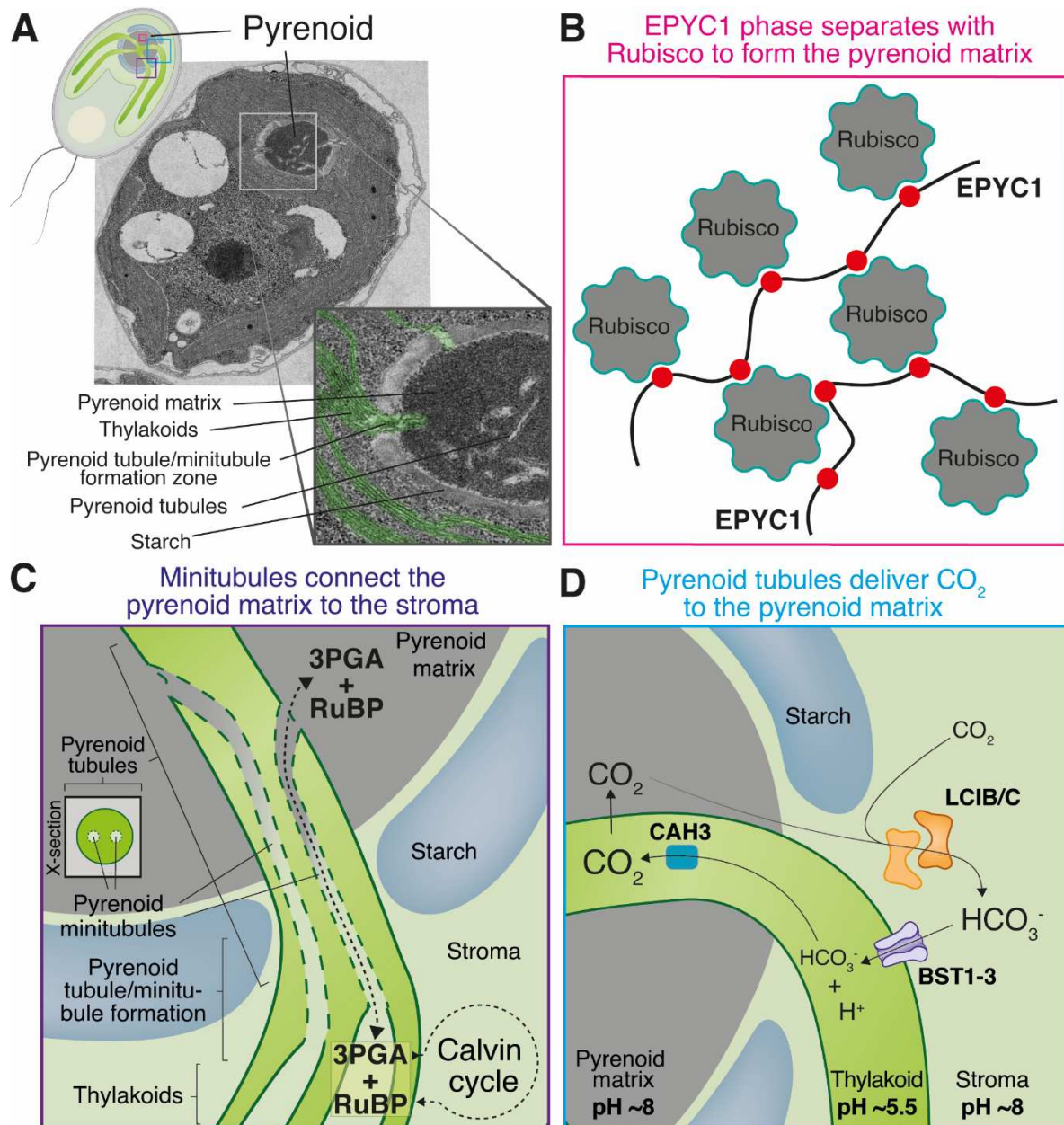
293 Although ultrastructural information is available for a wealth of species across diverse
294 lineages (see later section: *Pyrenoid structural diversity across different algal lineages*), our
295 most complete insights relating to pyrenoid form and function are for *Chlamydomonas*.
296 Detailed three-dimensional structural information of the pyrenoid obtained by ion beam milling
297 cryo-electron tomography (cryo-ET; [79]), quick freeze deep-etch electron microscopy
298 (QFDEEM; [51]) and pyrenoid protein fluorescence localization [80], have significantly
299 enhanced our understanding of pyrenoid architecture (Figures 3 and 4). Further, proteomics
300 of pyrenoid-enriched fractions have revealed the complex composition of the pyrenoid,
301 containing at least 190 different proteins, many of which remain uncharacterized [51, 81]. An
302 integrated localization and interaction study also indicated a large number of pyrenoid
303 components (89), many of which have been localized at sub-pyrenoid resolution [80]. Although
304 many different proteins have been localized to the pyrenoid, proteomic analysis shows the
305 pyrenoid matrix consists mainly of Rubisco molecules (~600 μM matrix concentration; [36])
306 and the intrinsically disordered linker protein EPYC1, that is essential for condensation of
307 Rubisco to form the pyrenoid matrix (Figure 4B) [36, 51]. Here, Rubisco functions within the
308 Calvin-Benson-Bassham (CBB) cycle, with strong evidence supporting that it is the only CBB
309 enzyme partitioned within the pyrenoid [82].

310 In addition to the pyrenoid matrix, traversing thylakoid tubules form a characteristic
311 star-shaped network within the pyrenoid. *In situ* cryo-ET in *Chlamydomonas* has revealed the
312 intriguing complexity of thylakoid membrane organization and structural changes as it enters
313 the pyrenoid matrix. Thylakoid membranes outside of the pyrenoid are organized in multiple
314 parallel stacked membrane layers [83], which drastically change as they enter the pyrenoid
315 matrix through fenestrations in the transient stromal starch sheath. The membrane layers
316 merge into cylindrical structures, termed pyrenoid tubules, that advance through the pyrenoid
317 matrix and converge in the centre of the pyrenoid, forming an interconnected network of
318 smaller, shorter tubules [79]. Within pyrenoid tubules, minitubules form luminal conduits
319 between the chloroplast stroma and the pyrenoid matrix and based on their diameter (~3-4 nm
320 at matrix opening) have been proposed to facilitate exchange of ATP and CBB metabolites

321 (incoming Ribulose 1,5 bisphosphate (RuBP) and outgoing 3-phosphoglycerate (3PGA)) but
322 not proteins (Figure 4C) [51, 79, 82]. The wider lumen of the pyrenoid tubules is continuous
323 with the thylakoid lumen and is postulated to transport HCO_3^- towards the centre of the
324 pyrenoid, following channelling from the chloroplast stroma into the thylakoid lumen through
325 bestrophin-like channels [84]. Central to CO_2 delivery is the carbonic anhydrase, CAH3, that
326 catalyses the dehydration of HCO_3^- to CO_2 in the acidic lumen of the pyrenoid tubules. This
327 process enables CO_2 diffusion across the tubule membrane into the pyrenoid matrix for fixation
328 by Rubisco (Figure 4D). CAH3 has been localized to the pyrenoid tubules and a *cah3* mutant
329 has a defective CCM, despite accumulating inorganic carbon at higher concentrations than
330 wild-type [11, 85-87]. There is strong evidence that the pyrenoid tubules also differ in their
331 protein composition from the rest of the thylakoid membrane. Immunogold labelling and
332 photosystem (PS) I and PSII activity assays suggested that the pyrenoid tubules contain active
333 PSI but not PSII [88]. However, recent fluorescent protein tagging of several photosystem
334 proteins revealed that subunits of both photosystems are present in the tubules, indicating that
335 partially-assembled or inactive PSII may be present [80]. Strikingly, some PSI subunits e.g.
336 PSAH are even enriched in the tubules. The functional implications of these
337 depletion/enrichment patterns are yet to be experimentally shown but could be related to
338 reducing photorespiration by minimizing O_2 release within the pyrenoid through photosynthetic
339 H_2O splitting at PSII reaction centres. However, collectively, these observations highlight the
340 importance of membrane traversions in the metabolic fluxes of the pyrenoid and suggest an
341 important role in its photosynthetic operation.

342

343



344
 345
 346
 347
 348
 349
 350
 351
 352
 353
 354
 355
 356
 357
 358
 359
 360
 361

Figure 4. The *Chlamydomonas* pyrenoid is at the heart of the CO₂ concentrating mechanism and enables efficient CO₂ fixation. **A)** TEM image of *Chlamydomonas reinhardtii* grown in light and under air levels of CO₂ where a complete pyrenoid is assembled. Zoom highlights key structural parts of the pyrenoid. Thylakoids false coloured green for clarity. Top left diagram is for orientation of panels B-D. **B)** The pyrenoid matrix is predominantly composed of Rubisco-EPYC1 condensate. Multiple Rubisco binding regions on EPYC1 enable complex coacervation with the Rubisco holoenzyme which is a hexadecameric assembly of 8 large and 8 small subunits. **C)** As thylakoids enter the pyrenoid they form pyrenoid tubules. Minitubules (dashed lines) form within the pyrenoid tubules and connect the pyrenoid matrix to the stroma. They are postulated to enable the large flux of metabolites in and out of the pyrenoid. Inset: cross-section (X-section) of minitubules within a pyrenoid tubule. **D)** Pyrenoid tubules are proposed to deliver CO₂ to Rubisco in the pyrenoid matrix. Current data supports that HCO₃⁻ enters from the stroma into the thylakoid lumen via bestrophin-like channels. In the acidic lumen HCO₃⁻ is converted to CO₂ via CAH3 and subsequently diffuses into the pyrenoid matrix. LCIB/LCIC is proposed to convert stromal CO₂ to HCO₃⁻ via active CO₂ uptake and CO₂ recapture from the pyrenoid. Minitubules are not shown for clarity.

362 The *Chlamydomonas* pyrenoid is surrounded by a sheath that is composed of several
363 starch plates. The starch sheath develops rapidly under limiting CO₂ concentrations [89] and
364 has been proposed to act as a diffusion barrier to reduce the loss of CO₂, that diffuses readily
365 between the stroma and matrix [73]. Although it has been suggested that the absence of the
366 starch sheath does not affect photosynthetic productivity [90], recent studies indicate a
367 correctly formed starch sheath is required for normal pyrenoid formation and the operation of
368 an efficient CCM [42, 91]. In addition to starch, the sheath also contains several proteins.
369 These proteins appear to be distributed uniformly over the starch plates, or localized in distinct
370 puncta or meshes in close proximity to the starch plates [80]. The functional implications of
371 these different distribution patterns remain unclear, but their positioning appears to be
372 important for CCM function [91]. A subset of proteins that localize in a plate-like pattern are
373 predicted to function as starch-branching enzymes, whereas the mesh distributed proteins
374 appear to fill the gaps between the starch plates, indicating a potential structural function [80].
375 Recently, a predicted starch-binding Rubisco-interacting protein, SAGA1 (StArch Granules
376 Abnormal 1), that localizes to distinct puncta at the pyrenoid matrix/starch interface was shown
377 to affect pyrenoid number and sheath morphology [42]. Interestingly, the two carbonic
378 anhydrase homologs, LCIB and LCIC, that are recruited to the pyrenoid in very low CO₂
379 concentrations (<0.02% CO₂) are also localized in distinct puncta but on the external surface
380 of the starch sheath [80, 92], where they are expected to minimize the loss of CO₂ from the
381 pyrenoid by converting emanating CO₂ back to HCO₃⁻, that can be readily concentrated again
382 (Figure 4D) [93]. LCIB homologs show *in vitro* carbonic anhydrase activity, however this could
383 not be demonstrated for the *Chlamydomonas* LCIB/LCIC proteins [94], potentially indicating
384 the absence of critical regulatory subunits or that activity requires specific cellular conditions.
385

386 **EPYC1 links Rubisco to form the pyrenoid matrix**

387 In *Chlamydomonas*, the abundant, low CO₂-induced linker protein, EPYC1, underpins the
388 functional phase separation of Rubisco to form the pyrenoid [44, 51]. In mutants depleted of
389 EPYC1, Rubisco fails to aggregate and is dispersed in the chloroplast [51], resulting in a
390 deficient CCM [51]. EPYC1 is a low complexity, largely disordered ~35 kDa protein, consisting
391 of five near-identical repeats [44, 51, 95]. Each ~60 amino acid repeat contains a predicted α -
392 helix, and significant charge patterning [44, 51]. The high isoelectric point (pI) of EPYC1 (11.7)
393 establishes a net positive charge of the unmodified protein in the slightly basic pyrenoid matrix
394 (pH ~7-8.5), in both photosynthetic and non-photosynthetic conditions [36, 96]. As described
395 above, *in vitro* demixing assays have demonstrated that LLPS of Rubisco by EPYC1 occurs
396 via complex coacervation, in which both components are required [44]. In line with general
397 LLPS principles, demixing was also demonstrated to require multivalent interactions between
398 the Rubisco holoenzyme and EPYC1 [29, 97].

399 Prior to EPYC1 discovery and functional characterization, Meyer et al. [98]
400 demonstrated that the sequence composition of the surface-exposed α -helices of the Rubisco
401 Small Subunit (SSU) was conditional for *Chlamydomonas* pyrenoid formation. Wunder et al.
402 [44] confirmed the importance of this interface for *in vitro* demixing and suggested the
403 association could be dominated by charge interactions between negative patches of the SSU
404 α -helices and regions of patterned positive charge in EPYC1. Yeast two-hybrid (Y2H) data
405 confirmed the SSU α -helices are necessary for interaction with EPYC1, and that other SSU
406 features enhance this interaction [97]. In line with previous predictions [51], it was later
407 demonstrated that EPYC1's interaction with Rubisco is enhanced by its repeating helical
408 regions [97]. More recently, single particle cryo-electron microscopy of a complex of Rubisco
409 and a 24 amino acid EPYC1 peptide containing the helical region has outlined the structural

410 basis for this interaction, revealing a primarily electrostatic and hydrophobic interface [95]. The
411 peptide was bound to each of the SSUs of Rubisco, indicating the holoenzyme can bind one
412 of EPYC1's five helical regions up to 8 times. In the same study, mutation of EPYC1 interface
413 residues decreased demixing of Rubisco *in vitro* and Rubisco substitutions at the interface
414 prevented pyrenoid formation *in vivo*, confirming the role of this low affinity interaction in
415 condensation of Rubisco. It is proposed that consecutive binding regions of the full length
416 EPYC1 peptide can facilitate the low affinity, multivalent interactions with multiple Rubisco
417 molecules required for condensation into the pyrenoid matrix. Key to this model, is the ability
418 for the unstructured region between two adjacent helical regions to span the distance between
419 Rubisco holoenzymes in the pyrenoid. *In-situ* cryo-ET data indicates a median distance of ~4
420 nm between EPYC1 binding sites on adjacent holoenzymes [79, 95]. The ~40 amino acid
421 unstructured regions between the 5 binding regions of EPYC1 are proposed to facilitate the
422 spanning of this distance, with wormlike chain models indicating a minimal energetic cost (< 3
423 $k_b T$) for stretching [95].

424 EPYC1 displays functional similarity to CsoS2 and CcmM in cyanobacteria [43, 46, 47].
425 Both EPYC1 and CsoS2 utilise helical regions to contact Rubisco, whereas CcmM utilises a
426 Rubisco SSU-like globular domain. Although all three Rubisco condensation events appear to
427 be underpinned by a similar multivalent mechanism, the sequences of the Rubisco-interacting
428 regions of CsoS2 and CcmM bear no homology to each other nor EPYC1, suggesting a
429 convergent evolutionary mechanism. CsoS2 and CcmM concurrently contact both the large
430 and small subunits of the morphologically similar form I Rubisco holoenzyme (L_8S_8) in the
431 cyanobacterium *Synechococcus elongatus* and the chemoautotrophic proteobacterium
432 *Halothiobacillus neapolitanus* respectively [43, 47]. It is postulated that the concurrent binding
433 of CsoS2 and CcmM to both the Rubisco large and small subunits results in only fully
434 assembled and functional Rubisco holoenzymes being incorporated into the carboxysome [43,
435 47]. Current data suggests that EPYC1 may exclusively contact the small subunit [95].
436 Additionally, whereas CsoS2 and CcmM facilitate aggregation using only a portion of their full-
437 length sequence, EPYC1 appears to dedicate its full length to multivalent interactions with
438 Rubisco [43, 47]. Although it is expected that linker proteins facilitate phase separation of other
439 pyrenoids [99], the lack of obvious EPYC1 homologs suggests that analogous linker proteins
440 will display a range of sequence characteristics across pyrenoid lineages, especially outside
441 of the Archaeplastida (form IB Rubisco), where Rubisco forms are variant
442 (dinoflagellates/alveolata [form II], all other clades [form ID]). Predictions based on
443 characterized linkers, suggest that analogous proteins contain: a) regions of disorder that are
444 continuous and cover part, or all of the protein sequence; b) repeat motifs within this disordered
445 region that will interact with Rubisco using localized structure; c) patterning of charged
446 residues throughout the full-length protein; and d) low complexity amino acid sequences.
447 Mackinder et al. [51] predicted the presence of analogous proteins in four other species using
448 a search framework based on some of these constraints, but these are yet to be experimentally
449 validated. These observations, alongside data from green algae that pyrenoid presence is not
450 determined by SSU sequence [100], certainly suggest that the presence of analogous linker
451 proteins is probably widely determinant of pyrenoid formation across lineages.

452 Although considerable progress has been made to characterize the EPYC1-Rubisco
453 interaction, several questions remain outstanding. The average fraction of bound sites for both
454 EPYC1 and Rubisco are uncharacterized (Figure 5A). In addition, although EPYC1's helical
455 interaction is well defined, the behaviour of the flexible regions between the helices are largely
456 unassessed. In other condensates, the length and interactions of these flexible regions have

457 been demonstrated to affect assembly [33], and should be considered in future studies of
458 pyrenoid dynamics.

459

460 **A Rubisco-binding motif targets proteins to the pyrenoid and may guide pyrenoid** 461 **assembly**

462 Recent work has proposed a framework for pyrenoid assembly in *Chlamydomonas* [101].
463 Multiple pyrenoid localized proteins were shown to contain a conserved Rubisco-binding motif
464 (RBM). This RBM is repeated five times in EPYC1 and two or more times, including at the C-
465 terminal, in other confirmed pyrenoid localised proteins. The EPYC1 RBM forms part of the α -
466 helix that directly binds Rubisco [95]. The RBM is found in proteins with diverse structural
467 features including predicted transmembrane domains and predicted starch binding domains.
468 Two proteins that contain both RBMs and transmembrane domains (termed Rubisco binding
469 membrane proteins 1 and 2 [RBMP1/2]) specifically localised to the pyrenoid tubules. Whilst
470 two proteins containing RBMs and starch binding motifs, SAGA1/2, localized to the pyrenoid
471 matrix/starch interface. Fusion of the motif to both non-pyrenoid localised stromal and
472 transmembrane thylakoid proteins resulted in targeting to the pyrenoid matrix and pyrenoid
473 tubules respectively. An elegant assembly mechanism is suggested, in which RBMP1/2 tether
474 the Rubisco matrix to the pyrenoid tubules and that SAGA1/2 tether the starch sheath to the
475 matrix [101]. However, characterization of RBMP1/2 deletion mutants has yet to be completed
476 and there is contradictory evidence supporting the role of SAGA1 as purely a Rubisco
477 matrix/starch tether, with a SAGA1 mutant having a severely disrupted CCM, abnormal starch
478 and multiple pyrenoids [42]. It might be expected that a mutant where starch tethering is absent
479 would have a phenotype in line with a starchless mutant, which retains a canonical single
480 pyrenoid and has only a slightly defective CCM [91]. Further work is required to understand if
481 RBMs are purely for pyrenoid structural assembly (as in matrix assembly via EPYC1) or
482 whether it is a mechanism to target functional proteins to specific sub-pyrenoid regions (Figure
483 5A).

484

485 **Pyrenoid assembly around membranes and pyrenoid tubule formation**

486 Pyrenoids are one of two identified LLPS organelles that are crossed by a membrane system.
487 The others are sponge bodies, organelles so far only observed in germline cells of *Drosophila*
488 *melanogaster* and *Caenorhabditis elegans* [102]. Sponge bodies are ribonucleoprotein
489 granules found in the cytoplasm, which are crossed by multiple ER cisternae [103, 104]. The
490 function of sponge bodies remains unclear. Even though membrane traversal of LLPS
491 organelles is rarely observed so far, several interactions between LLPS organelles and
492 membranes have been reported, where the membraneless organelle is directly attached to a
493 membrane. These include: T cell and other receptors [105, 106]; nuclear pore complexes
494 [107]; ribonucleoprotein granules such as P-bodies, stress granules and TIS granules that
495 interact with the ER [108, 109]; the yeast pre-autophagosomal structure that is attached to
496 the vacuole [110]; and the protein synapsin, which can phase separate and recruit lipid
497 vesicles to the droplets *in vitro* [111]. This broad range of reported interactions between
498 membraneless organelles and membranes imply that these interactions are quite common
499 and play a role in various biological processes. For some LLPS organelles that are attached
500 to a membrane, there is evidence that proteins often function as tethers. For instance, the pre-
501 autophagosomal structure of yeast is tethered to the vacuole via protein-protein interactions
502 between several intrinsically unfolded proteins of pre-autophagosomal structure and tonoplast
503 membrane proteins [110]. This would support the role of RBMP1/2, or other transmembrane
504 containing Rubisco interacting proteins, functioning as pyrenoid matrix membrane tethers.

505 However, other pyrenoid tubule membrane attachment mechanisms are feasible, including the
506 recently demonstrated sensing and direct binding to curved membranes of intrinsically
507 disordered region containing proteins [112, 113] or interactions between pyrenoid proteins and
508 the presumably unique lipid bilayer properties of the pyrenoid tubules.

509 Whereas some progress is being made on pyrenoid matrix interactions with thylakoid
510 membranes, we know little about the thylakoid tubules within the pyrenoid. The thylakoid
511 membrane in photosynthetic organisms, from which the tubules derive, differs in several
512 respects from other membrane systems. It has an unusual lipid composition and consists of
513 almost 80% uncharged galactolipids, ~10% anionic sulpholipids and ~10% anionic
514 phospholipid [114]. Due to a high content of hexagonal phase forming lipids (~60% of the total
515 lipid), the thylakoid membrane is highly curved. There is no data on the lipid content of pyrenoid
516 tubules versus the bulk thylakoid membranes, although the typical further increased curvature
517 of pyrenoid tubules could result in specific lipid partitioning. Moreover, the thylakoid membrane
518 has a high protein content, with about 70% of the membrane surface occupied by proteins in
519 land plants [115]. The proteins are unevenly distributed over the thylakoid membrane, with
520 some proteins enriched in certain regions of the membrane, while depleted in others [83, 116].
521 Specifically, the two photosystems (PS) are heterogeneously distributed, with certain regions
522 where only PSI resides and others where only PSII is present. Similarly, the protein content of
523 the thylakoid tubules that traverse the pyrenoid differs from the other regions of the thylakoid
524 membrane across algal lineages [55, 80, 88, 117, 118]. Some protein variation could be
525 explained by specific targeting of RBM containing transmembrane proteins to the pyrenoid
526 tubules [101], but distribution variation in many proteins that lack RBMs, such as PSI and PSII
527 subunits, is unknown.

528 In addition, the biogenesis of the pyrenoid tubules and minitubules remains completely
529 unresolved. In many algal species, the thylakoid membrane drastically changes as it enters
530 the pyrenoid matrix. In *Chlamydomonas*, the stacked membrane layers of the thylakoid
531 membrane merge into one cylindrical tubule per stack that engulfs smaller minitubules as they
532 approach the pyrenoid (Figure 3 and 4; [51]). In the centre of the pyrenoid these tubules merge
533 to form an interconnected network. The factors that transform the thylakoid membrane from
534 multiple stacked membrane layers into highly curved tubules remain unknown. Recently, it has
535 been shown that LLPS on the surface of liposomes can lead to the formation of invaginations
536 in the liposomes that can develop into lipid tubules [119]. However, in pyrenoid-less
537 *Chlamydomonas* strains (where the Rubisco SSU is exchanged for the SSU of higher plants,
538 which do not bind EPYC1) the pyrenoid tubule network in the centre of the chloroplast seems
539 largely unaffected in TEM images. This suggests that LLPS on the membrane surface is not
540 responsible for the formation of the pyrenoid tubules and the pyrenoid tubules might form
541 independently from pyrenoid matrix assembly [120]. Yet, we lack high-resolution 3D images
542 of the tubule network in these strains to ensure that the network is not altered in any way due
543 to the absence of the pyrenoid matrix. Even though it seems plausible that the pyrenoid matrix
544 is involved in formation and shaping of the pyrenoid tubule network it seems likely that
545 membrane fusion/fission and curvature inducing proteins, which are also involved in thylakoid
546 biogenesis [121], are part of these processes.

547

548 **PYRENOID DYNAMICS**

549

550 The pyrenoid of *Chlamydomonas* displays many of the characteristics of LLPS bodies, with
551 both *in vivo* [36] and *in vitro* [44] studies providing multiple levels of support. This section will
552 outline this supporting evidence and highlight our current state of knowledge and open

553 questions related to pyrenoid dynamics including division, regulation of pyrenoid LLPS, and
554 pyrenoid nucleation. Whereas most of our experimental data comes from *Chlamydomonas*,
555 decades of observations across diverse algae provide translational insights into pyrenoid
556 dynamics.

557

558 **Evidence for Pyrenoid LLPS**

559 Thanks to the work of Freeman Rosenzweig et al. [36], some of the classical hallmarks of
560 liquid droplets initially described by Brangwynne et al. [24], including fusion, dissolution, *de*
561 *novo* formation and internal rearrangement, have all been observed over second timescales
562 in the *Chlamydomonas* pyrenoid. In this study, *in situ* cryo-ET also revealed that Rubisco
563 molecules in the pyrenoid exhibit short-range distribution patterns, characteristic of liquid-like
564 order. The additional *in vivo* observations that pyrenoids adopt a largely spherical morphology
565 that can be reversibly deformed and appears to be wetted to the surrounding starch sheath
566 provide additional fundamental support for the LLPS nature of the pyrenoid [122]. These *in*
567 *vivo* observations were bolstered by the work of Wunder et al. [44], who showed that a minimal
568 *in vitro* reconstituted pyrenoid matrix (Rubisco and EPYC1) possessed many similarities to its
569 *in vivo* counterpart over complementary timescales. Here it was demonstrated that functional
570 Rubisco could be demixed by the linker EPYC1 under physiologically relevant conditions and
571 concentrations in a valency-dependent manner. Further, fluorescence recovery after
572 photobleaching (FRAP) analysis indicated the reconstituted droplets rearrange over similar
573 timescales to those observed *in vivo* [36], and thus provide a suitable proxy for the LLPS of
574 the pyrenoid.

575

576 **Pyrenoid inheritance**

577 During mitotic division of vegetative cells, approximately two thirds of *Chlamydomonas*
578 daughter cells inherit pyrenoids via fission, with the remaining daughter cells either
579 asymmetrically inheriting the whole mother-cell pyrenoid (~20%), forming a *de novo* pyrenoid
580 from dilute stromal Rubisco (~6%) or failing to inherit a pyrenoid (~8%) [36]. Fission [123] and
581 *de novo* [124-126] pyrenoid inheritance are classically described in green algae, but have also
582 been described in hornworts and non-green lineages (fission: [127-130]; *de novo* assembly:
583 [131-136]), where both mechanisms appear equally prevalent. Besides *Chlamydomonas*,
584 multiple concurrent pyrenoid inheritance mechanisms have only been reported in
585 *Arachnocyrtis demoulinii* sp. nov. (stramenopila; [39]) and *Chlorogonium elongatum*
586 (chlorophyta; [137]). It is unlikely this is unique to these species and is instead likely reported
587 due to more intensive characterizations. Anecdotally, *de novo* pyrenoid formation following
588 division appears to be reported more commonly in species where vegetative cells possess
589 multiple distinct pyrenoids. This observation appears to extend across lineages, but exceptions
590 do exist in some chlorophyta [138, 139] and the definition of 'multiple pyrenoids' becomes
591 unclear, especially in multicellular hornworts [140]. Pyrenoid fission is typically induced by
592 plastid constriction, or less commonly, starch sheath invagination [123]. With pyrenoid fission
593 driven by plastid constriction being documented across lineages: green algae (chlorophyta)
594 [141], haptophytes (haptophyta) [142], hornworts (bryophyta) [130, 143], diatoms
595 (stramenopila) [144, 145], brown algae (stramenopila) [131, 146], red algae (rhodophyta) [129,
596 147] and dinoflagellates (alveolata) [148].

597 In *Chlamydomonas*, fission occurs over an ~7 minute window at the end of the
598 chloroplast division (~30-80 minutes), suggestive of a mechanical interference by the plastid
599 cleavage furrow [36], consistent with the observations of Goodenough [141]. The cleavage
600 furrow advances across a symmetry axis that is important for maintaining the polarity of the

601 cell following cytokinesis [149, 150]. Chloroplast division in plants has been shown to be
602 synonymous with the widely conserved contraction of a stromal ring-like FtsZ structure [151,
603 152] positioned by MIN proteins [153], presumably inherited from cyanobacterial ancestors
604 [154]. Homologous systems are present in algae [139, 155-158], but there is little clarity on
605 their roles in plastid division mainly due to lack of conserved transcriptional patterning [157,
606 159-161], and formation of multiple conglomerate FtsZ rings [162, 163]. F-actin has also been
607 implicated in facilitating furrow progression at the chloroplast to aid subsequent chloroplast
608 division in *Chlamydomonas* [164] and two species of red algae [165, 166], where it could
609 provide a structural signal [167, 168], but this role is hypothetical. Clearly more work is required
610 to definitively determine the forces driving plastid division in algae, and the implications this
611 has on cleavage furrow progression and pyrenoid fission. Whether furrow-induced pyrenoid
612 fission is underpinned by molecular interactions or is the result of a purely mechanical
613 interference also remains to be seen. The dynamic distribution of pyrenoid ultrastructural
614 features (starch and thylakoid material) throughout division is unassessed in *Chlamydomonas*,
615 and has been sparsely reported in other pyrenoid-containing species. In *Leptosiropsis torulosa*
616 (chlorophyta) however, the starch is reported to divide between daughter pyrenoids from the
617 mother [169]. Given the apparent importance of starch in form and function of the pyrenoid, it
618 is likely that coordinated distribution of starch (when present) through divisions is equally
619 important [42, 91]. In *Porphyridium cruentum* (rhodophyta) the traversing thylakoid material is
620 divided between the daughter cells [127]. Likewise, Lokhorst and Star [170] report even
621 distribution of both starch and thylakoid structures through pyrenoid fission in *Ulothrix*
622 (chlorophyta). The canonical positioning of the pyrenoid at the tubule network suggests that
623 symmetrical segregation of this network between daughter cells will be equally important for
624 correct pyrenoid retention and reformation through cell division [51].

625 Intriguingly, in *Chlamydomonas* towards the end of chloroplast division and prior to
626 pyrenoid division under constant light, a significant portion (~35-50%) of the Rubisco/EPYC1
627 disperses from the pyrenoid into the surrounding stroma [36]. It is expected that this dispersion
628 will reduce pyrenoid viscosity and surface tension and accordingly reduce the mechanical
629 force required for pyrenoid fission by the centrally positioned cleavage furrow, in line with
630 physical theory [171]. Freeman Rosenzweig et al. [36] also note, in cell divisions where the
631 pyrenoid does not appear to be bisected during cytokinesis, pyrenoid fission is not observed.
632 This might suggest a primarily mechanical driving force for fission, but it is possible that
633 incorrect segregation of unresolved ultrastructural features also play a role. The interference
634 of the cleavage furrow on pyrenoid ultrastructure is not well studied, but the classical
635 observations of the green algae *Tetracystis isobilateralis* by Brown et al. [172] suggest a role
636 for pyrenoid traversing chloroplast thylakoids in division. A thylakoid membrane-oriented
637 pyrenoid division mechanism is plausible given the recent reports of endoplasmic reticulum
638 membrane contact with liquid droplet P-bodies in directing their fission location and propensity
639 [108]. Collectively, the above observations highlight the importance of the canonical
640 positioning of the pyrenoid and cleavage furrow during cell division to facilitate pyrenoid
641 inheritance through fission. When either of these positional requirements are awry, pyrenoid
642 fission does not occur, and one of the daughter cells inherits the mother pyrenoid, leaving its
643 sister pyrenoid-less. In the pyrenoid-less daughter cell, ~50% form pyrenoids *de novo* from
644 coalescence or apparent Ostwald ripening of multiple incipient pyrenoid puncta in the
645 chloroplast stroma [36], similar to descriptions in hornworts [173]. The sites of *de novo*
646 formation are not well described, but the observations of Bisalputra and Weier [174] suggest
647 an interplay with thylakoids in other species. These observations suggest an important role for
648 thylakoid membranes in pyrenoid division and *de novo* assembly.

649 In addition to facilitating pyrenoid fission, the relocation of Rubisco and EPYC1 to the
650 chloroplast stroma may have evolved as a safeguard to provide a basal level of Rubisco to the
651 daughter cells for rapid *de novo* pyrenoid formation in the absence of fission [36], similar to P
652 granule relocation by re-condensation [24]. This has been proposed to facilitate Rubisco
653 inheritance through division in the multiple pyrenoid-containing cells of hornworts [140], and is
654 a plausible explanation for the observation of common *de novo* formation in other multiple
655 pyrenoid-containing species, where coordination of furrow-induced fission is more difficult. The
656 lack of high-resolution studies outside of the green lineage makes translation of these
657 observations difficult, and it is possible diverse pyrenoid-containing species operate distinct
658 pyrenoid distribution mechanisms. Even in *Chlamydomonas* there are multiple open questions
659 (Figure 5), such as: What happens to pyrenoid ultrastructural features throughout division?
660 What determines plastid fission and cleavage furrow positioning? What determines the site of
661 *de novo* pyrenoid assembly? Is the basis for fission solely mechanical?
662

663 **Regulation of pyrenoid dynamics**

664 Although the dynamic, liquid-like properties of the *Chlamydomonas* pyrenoid have been well
665 characterized, very little is known about their regulation. In this section, we discuss the possible
666 regulatory mechanisms at play (summarised in Figure 5B), relating existing pyrenoid data and
667 the wealth of control mechanisms demonstrated in other biomolecular condensates (see
668 Dignon et al. [30] and Owen and Shewmaker [35] for recent reviews). As discussed previously,
669 the pyrenoid exhibits several apparent phase transition events that occur over different
670 timescales, and we discuss their potential control mechanisms accordingly.
671

672 **Pyrenoid dynamics over short timescales**

673 The rapid nature of pyrenoid dynamics throughout cell division (dissolution and *de novo*
674 formation) has generated considerable interest in the role of post-translational modifications
675 (PTMs) through these events [36], given widespread reports of their role in regulating
676 analogous condensates [35, 175]. Given that intrinsically disordered proteins are frequently
677 modified post-translationally due to their conformational accessibility [176], it appears probable
678 that PTM of EPYC1 will play a role in pyrenoid dynamics. Although PTMs of globular domains
679 are more sparsely reported in coacervation control, with reports limited to ribonucleoprotein
680 granule component TDP-43 [177], here we also discuss the possibility of PTM of Rubisco to
681 effectively modulate valency and, thereby, control the size and physical properties of the
682 aggregate. These considerations are made under the assumption that matrix components
683 (Rubisco/EPYC1) are readily modified both within the dilute stromal and condensed matrix
684 states, as has been described in other ‘active’ condensates [178, 179].
685

686 Phosphorylation: Given that many biomolecular condensates incorporate phosphatases and
687 kinases that regulate the phosphorylation state and essential interactions of component
688 molecules that ultimately determine phase dynamics [29], there is considerable interest in
689 exploring the phospho-states of pyrenoid matrix components. The rapidly achieved, highly
690 phosphorylated state of EPYC1 in light under low CO₂ (where nearly all Rubisco is condensed
691 in the pyrenoid) conditions [180, 181] has led to suggestions that the phosphorylation state of
692 EPYC1 may control phase separation, by affecting Rubisco binding valency [80, 182]. Turkina
693 et al. [180] showed that phosphorylation of EPYC1 in response to CO₂ limitations occurs at
694 serine and threonine residues within the flexible regions between the Rubisco interaction
695 helices [95, 97, 183]. Alongside tyrosine, phosphorylation of serine/threonine residues has
696 been shown to both enhance and hinder phase separation dynamics in other systems, through

697 recruitment and interaction screening effects respectively [35]. Here we discuss the role of
698 phosphorylation-enhanced valency, given the correlation with pyrenoid formation, but
699 acknowledge the absence of definitive evidence.

700 Interaction data supports EPYC1 association with two 14-3-3 phospho-binding
701 proteins, FTT1 and FTT2 [80]. 14-3-3 proteins are highly conserved proteins that are
702 implicated in a multitude of biological phosphorylation regulated processes across the
703 eukaryotic tree of life [184, 185], with diverse and often contradictory functions, including
704 protein binding occlusion, induced conformational change and interaction scaffolding [185].
705 14-3-3 binding potentially occurs at one of EPYC1's phosphorylated serine residues that
706 resides within an almost complete 14-3-3 binding motif ([R].[S].[X].[pS].[X].[P] [186]), that is
707 repeated 3 times within the EPYC1 sequence [186]. Given the phosphorylation state of
708 EPYC1, 14-3-3 proteins would therefore be expected to be bound in low CO₂ conditions, and
709 may explain low CO₂ dependent pyrenoid formation potentially through interaction scaffolding
710 by increased linker protein valency or self-association, as observed in other complex
711 coacervates [187, 188].

712 Besides a potential 14-3-3 binding role, our understanding of EPYC1 phosphorylation
713 effects is limited. No interacting pyrenoid kinases or phosphatases were highlighted from
714 interactome studies [80], and our understanding of the effects of phosphorylation on the
715 EPYC1-Rubisco interaction are lacking. The presence of the phosphorylation sites outside of
716 the interacting regions of EPYC1 might suggest that there is no large impact on the interaction
717 with Rubisco. Equally, modifications within flexible regions have been shown to enhance
718 phase separation in other condensates [32, 187], but our understanding here is sparse. A
719 detailed study of EPYC1 phosphorylation, that highlights potential kinases/phosphatases and
720 assesses the Rubisco interaction would provide insight into the correlated process of pyrenoid
721 formation and EPYC1 phosphorylation.

722
723 Methylation: Residue-specific methylation has also been shown to have wide-reaching effects
724 on droplet formation in other systems, primarily through arginine-associated modifications [35].
725 Two candidate methyltransferases have been implicated in the CCM, and we discuss these
726 separately below. Although these methyltransferases are predicted to act on lysine, its
727 similarity to arginine and the apparent monomethylation of lysine at three sites in EPYC1 under
728 low CO₂ conditions warrant its consideration in pyrenoid dynamics [80]. Mutants of the first
729 methyltransferase, CIA6, fail to form a canonical pyrenoid and exhibit growth phenotypes
730 similar to the mutant of the linker protein, EPYC1 (failed pyrenoid assembly and no CCM) [51,
731 189]. This phenotype presumably indicates reduced EPYC1 accumulation, or a reduced
732 interaction with Rubisco, given that Rubisco accumulates to the same level in this strain and
733 that CIA6 appears not to methylate Rubisco *in vitro*. Ma et al. [189] also demonstrate reduced
734 levels of CCM components in the *cia6* mutant, but do not assess EPYC1 accumulation.
735 Establishing the transcript and protein levels of EPYC1 in this mutant would facilitate
736 disentangling the two possibilities for failed pyrenoid formation here. Interestingly, EPYC1's
737 methylation sites lie within the 'SKKAV' motif that Wunder et al. [44] hypothesised could drive
738 EPYC1's interaction with negative patches of Rubisco. Although methylation does not affect
739 the charge of residues and would therefore be unlikely to disrupt these non-specific charge
740 interactions, methylation at these sites would presumably preclude residue-specific cation- π
741 interactions, that could otherwise enhance valency.

742 The second putative methyltransferase, SMM7, has been localized to the pyrenoid
743 matrix [80], and is significantly upregulated in low CO₂ conditions, unlike CIA6 [190, 191], but
744 no phenotypic data is available. SMM7 bears homology to calmodulin dependent METTL21

745 proteins that methylate molecular chaperones to regulate their activity [192]. However, there
746 is currently no evidence to support this function for SMM7. Phenotypic analysis of SMM7
747 mutants with respect to EPYC1/Rubisco accumulation and methylation profiles should be
748 completed to further probe the role of methylation in pyrenoid assembly. It is equally possible
749 Rubisco methylation could contribute to perturbations in pyrenoid assembly, but methylation
750 profiles of Rubisco are not currently available across phase transitions.

751
752 Other post-translational modifications: Other PTMs, including lysine acetylation, arginine
753 citrullination and poly(ADP-ribosylation) have been implicated in phase separation dynamics
754 [35], but these are unexplored in *Chlamydomonas*. The observation that recombinant EPYC1
755 can phase separate *in vitro*, presumably in the absence of physiological PTMs [44], may imply
756 that the above potential modifications are not major determinants in coacervate formation, but
757 may play a role in the disassembly process that occurs during cell division and acclimation to
758 high CO₂ environments.

759

760 **Pyrenoid dynamics over longer timescales**

761 In contrast to the rapid pyrenoid phase transitions that occur prior to, and following cell division,
762 those that occur in response to CO₂ [193] and light [194] changes potentially occur over
763 significantly longer timescales (several hours). Although it is likely that PTMs play a role in the
764 regulation of these transitions, here we discuss the influence of global changes in cellular
765 physiology that could explain the slower response and have been implicated in the transitions
766 of other systems. These include pH [195, 196], temperature [197, 198], salt concentrations
767 [197] and osmotic pressure [199].

768

769 pH: The pH of the stroma markedly increases under light-dependent photosynthetic conditions
770 in higher plants [96], cyanobacteria [12] and algae [200], due to the pumping of protons from
771 the stroma into the thylakoid lumen. Under extended dark conditions the pyrenoid of
772 *Chlamydomonas* dissolves and Rubisco transiently relocates to the stroma [194]. The
773 correlation of photosynthetic stromal pH change and pyrenoid presence across light conditions
774 warrants interest in the effects of these changes on pyrenoid formation and function. In
775 cyanobacteria and algae, the photosynthetic pH rise increases the prevalence of HCO₃⁻ over
776 CO₂ in the stroma, and likely enhances CCM efficiency using specialized HCO₃⁻
777 transporters/channels that increase flux to Rubisco condensates [201]. Given the non-
778 membrane bound nature of the pyrenoid, it is expected that stromal pH increases (from ~7 in
779 the dark to ~8.5 in the light) will be mirrored in the pyrenoid matrix, with only slight variations
780 due to localized diffusive fluxes [96]. pH changes of this magnitude (~1.5 pH units) have been
781 shown to influence charge interactions by protonation/deprotonation of clustered charged
782 residues in the “pH sensor” domain of Sup35, where upshifted pK_a values are thought to
783 contribute a pH-sensitive function at physiological pH [196]. A similar process may promote
784 Pub1-directed pH-dependent stress granule assembly [202].

785 The Rubisco-interacting helices and ‘SKKAV’ motif represent the main charge
786 clustering in the EPYC1 sequence and could contribute a similar function in *Chlamydomonas*.
787 Alternatively regions of negative charge on the surface of the Rubisco SSU highlighted by
788 Wunder et al. [183] could behave similarly, especially given the more notable shift in pK_a of
789 residues in local charge regions of globular proteins [203]. However, although electrostatic
790 screening effects have been probed *in vitro* [44], the pH-sensitivity of EPYC1-Rubisco
791 demixing remains uncharacterized.

792

793 Concentration of pyrenoid components: The concentration of proteins and their associated
794 valencies clearly defines condensate assembly and composition [22]. Many primary pyrenoid
795 matrix components are differentially abundant across the light-dark and low-high CO₂
796 transitions, in correlation with the dissolution/relocalization of the pyrenoid and its components
797 [51, 194]. Certainly, the timescale for protein expression could provide a time-appropriate
798 explanation for the apparent slower pyrenoid dynamics observed across these transition
799 periods.

800 Both the Rubisco large and small subunits are consistently abundant throughout the
801 light-dark and low-high CO₂ transitions which would negate a concentration-dependent role
802 for them [194]. Contrastingly, EPYC1 displays differential abundance at both the transcript and
803 protein level across both the light-dark and low-high CO₂ transitions [51, 180, 190]. It is
804 possible these abundance changes could drive phase transitions observed *in vivo*, consistent
805 with linker concentration-dependent demixing effects observed in analogous systems [187].
806 Although protein abundance has been charted well across these transitions, the distinct
807 mechanisms of transcriptional control, cytoplasmic shuttling, chloroplast import and
808 degradation of EPYC1 are unexplored (Figure 5). These processes are undoubtedly entangled
809 with the aforementioned molecular modifications, but their interdependence and implications
810 remain unelucidated.

811
812 Temperature: Temperature is not likely to markedly affect pyrenoid formation and division
813 dynamics, given the low CO₂, pyrenoid-dependent growth of *Chlamydomonas* across wide
814 temperature ranges [204]. In line with this observation Wunder et al. [44] also reported no
815 significant shift in phase diagram across a range of physiologically relevant temperatures (0-
816 40 °C) for *in vitro* Rubisco-EPYC1 demixing. At a superficial level, the pyrenoids of cold-water
817 species are largely ultrastructurally similar to those of temperate species (for examples see
818 references [205-209]), indicating no major change in pyrenoid assembly.

819 It will be interesting to consider the characteristics of pyrenoids that form in cold-
820 adapted species such as *Chlamydomonas* sp. UWO241, where photosynthesis is adapted to
821 exhibit comparable rates to species grown at ambient conditions [210, 211]. Whether
822 pyrenoids in cold-adapted species exhibit the same dynamic properties observed in temperate
823 pyrenoid species is unknown. It has been reported that the linker protein EPYC1 is
824 downregulated during low CO₂ cold adaptation in *Chlamydomonas* [212], but whether this has
825 functional implications is unknown. In *Anthoceros* hornworts, pyrenoid shape has been
826 reported to change in response to cold-adaptation, from spindle-shaped to round [135],
827 perhaps suggesting an active process underpins maintenance of the spindle shape. These
828 observations likely suggest that temperature does not play a unique role in pyrenoid dynamics,
829 but study of matrix properties in cold-adapted species would nevertheless provide valuable
830 insight into the role of macroscopic properties (surface tension, viscosity) on pyrenoid function.

831
832 ATP and Ionic strength: Given the largely active state of many condensates in maintaining
833 their liquid-like properties through enzymatic processes [179], ATP concentration has been
834 proposed to play a role in biological phase separation events [30], given its role as a biological
835 hydrotrope [213]. As discussed previously, the ultrastructure of the pyrenoid has been
836 proposed to allow the exchange of ATP with the chloroplast stroma, facilitating activity of the
837 highly active canonical AAA+ ATPase chaperone, Rubisco activase (RCA) [214], amongst
838 other enzymes [79]. The presence of active PSI, and its associated cyclic electron transport
839 processes inside the pyrenoid could provide an alternative source of ATP for these processes
840 [80, 88]. RCA remodels Rubisco in the pyrenoid [215], and its ATP-consumptive activity is

841 related to the photosynthetic state of the cell [216]. In *Chlamydomonas*, RCA is located in the
842 pyrenoid [80, 217], where it has similar mobility to RBCS1, presumably to enable its dynamic
843 role [36]. It is possible that this presumably large change in flux of ATP when the photosynthetic
844 state of the cell changes plays a role in phase dynamics. However, pyrenoid phase dynamics
845 in response to flux changes in ATP and other key metabolites (RuBP, 3PGA, HCO₃⁻) are
846 largely unassessed in *Chlamydomonas*.

847 Similar to ATP-dependent dynamics, ionic strength has been implicated in disassembly
848 of analogous condensates, where electrostatic interactions dominate [197]. Notably, the *in*
849 *vitro* demixing of the N-terminal domain of α -carboxysome linker CsoS2 with Rubisco requires
850 low salt concentration [43], analogous to the salt-dependent demixing of EPYC1 and Rubisco.
851 In addition to the proposed pH-dependent effects on electrostatic interactions in the pyrenoid,
852 spatiotemporal Ca²⁺ fluxes provide an additional layer of charge effects. CAS1, a Ca²⁺-sensing
853 protein, re-localizes to the pyrenoid upon CCM induction, possibly facilitating a CO₂ response
854 that facilitates assembly of key CCM components [218, 219]. It was also determined that
855 pyrenoid Ca²⁺ concentration is markedly increased in low CO₂ conditions [218]. The increased
856 Ca²⁺ concentration would presumably screen electrostatic interactions and subsequently
857 disfavour phase separation of the pyrenoid. Whether these charge fluxes definitively affect the
858 putative electrostatic interaction between Rubisco and EPYC1 in the pyrenoid matrix is
859 undetermined, but electrostatic dependence of demixing is readily observed [44]. *In vivo*
860 quantification of ionic strength in the pyrenoid, using established methods [220], could provide
861 useful insight here.

862

863 **Pyrenoid size**

864 Pyrenoid size increases following division due to Rubisco recondensation and likely increases
865 due to CCM-induced relocalization [36, 194]. Across mature *Chlamydomonas* cells pyrenoid
866 size is largely consistent under the same growth conditions and appears to scale with cell size
867 during growth [42, 51, 221]. Rubisco-EPYC1 droplets are not size-limited *in vitro*, suggesting
868 that pyrenoid size is component limited *in vivo* [44], as observed in other biomolecular
869 condensates [25]. Alternatively, physical restrictions determined by other ultrastructural
870 features (starch/thylakoids) could limit droplet size. In a multiple pyrenoid-containing mutant of
871 the starch-associated Rubisco-binding protein SAGA1, the total pyrenoid matrix area is
872 decreased (indicating that pyrenoid volume is also decreased) despite Rubisco levels
873 remaining unaffected [42]. Thus, indicating that disrupted interactions between the pyrenoid
874 matrix and the starch has an effect on pyrenoid number and matrix area, however it has to be
875 noted that the exact functional role of SAGA1 is still unclear and similar multiple pyrenoid
876 phenotypes are also seen in EPYC1 and CIA6 mutants. At a biophysical level, the implications
877 of pyrenoid size relating to macroscopic properties, such as surface tension and viscosity are
878 unexplored.

879

880 **Pyrenoid dissolution**

881 High resolution spatiotemporal data is lacking for *Chlamydomonas* pyrenoid dissolution across
882 the slower low CO₂ to high CO₂ and light to dark transitions, though partial dissolution prior to
883 cell division is characterized over an ~20 minute window [36]. In the closely related
884 ulvophyceae, *Ulva linza* and *Ulva intestinalis* (chlorophyta), dark-induced dissolution appears
885 to occur over many hours [222], with a similar result observed in *Scenedesmus acuminatus*
886 (chlorophyta) [223]. No data is available for high CO₂ transitions.

887 As aforementioned, it is likely the rapid phase transition observed prior to division is
888 regulated at the post-translational level and suggests fine control over phase dynamics within

889 the cell. Following pyrenoid dispersing phase transitions, a portion of the matrix is retained at
890 the canonical pyrenoid position (centred on the thylakoid network intersection) (Figure 5B)
891 [120, 194]. The retained portion contains both Rubisco and EPYC1 [36]. Interestingly, a similar
892 phenomenon is observed in the 'pyrenoid-less' *epyc1* mutant [51], where a portion of the
893 Rubisco is maintained at the stellate thylakoid network. QFDEEM data indicate this
894 aggregation has a lower packing density than the pyrenoid, presumably due to the absence of
895 EPYC1 driven Rubisco packaging [51]. The presence of RBMs found in several pyrenoid
896 components that localize to distinct sub-pyrenoid regions [101] may explain this residual
897 Rubisco matrix at the canonical pyrenoid position in the *epyc1* mutant.

898 Crucially, the fate of EPYC1 during dissolution is not determined, with possibilities
899 including degradation, dissolution into the stroma as monomers (or homo-multimeric
900 complexes) or dissolution into the stroma as small EPYC1-Rubisco heteromeric assemblies.
901 Given that Rubisco is consistently abundant throughout transitions, the level of EPYC1 protein
902 abundance is likely pivotal in determining pyrenoid reformation following dissolution. EPYC1
903 degradation rates over pyrenoid division and CCM state changes are yet to be characterized,
904 but could hold vital clues for the dissolution and re-condensation mechanisms of the pyrenoid
905 (Figure 5A).

906

907 **Pyrenoid nucleation**

908 Nucleation of phase separated condensates is crucial to their dynamic functions and cellular
909 positioning, and requires surmounting a kinetic barrier [19]. This process can occur
910 homogeneously through random fluctuations at non-defined locations, or heterogeneously at
911 pre-existing sites, where pre-assembly seeds droplet formation [25]. *De novo* formation of
912 pyrenoids in the stroma has been documented widely. Observations in *Chlamydomonas* show
913 that multiple proto-pyrenoid puncta can form *de novo* in the stroma of daughter cells. One of
914 these puncta appears to form at the canonical position of the pyrenoid in the chloroplast, and
915 over time grows to become the main Rubisco aggregation in the stroma, whilst the other
916 puncta diminish [36]. Very little is known about this process, but recent evidence provides
917 some insight.

918 Nucleation at the canonical pyrenoid position is perhaps explained by enhanced
919 Rubisco accumulation. In parallel to RBMP1/2 potentially acting as tethers of the pyrenoid
920 matrix to tubules, they could also play a pivotal role in the initial recruitment of Rubisco to the
921 pyrenoid tubules to drive pyrenoid assembly [101]. As described above, SAGA1/2 are
922 suggested to play a role in pyrenoid assembly through starch adherence to the pyrenoid matrix
923 [101], however the role of these starch-associated proteins should not be overlooked when
924 interrogating pyrenoid nucleation. SAGA1/2 belong to a suite of coiled-coil containing proteins
925 associated with the pyrenoid, many of which appear to associate with starch [42, 80]. The
926 association of coiled-coil domains has been shown to provide structural scaffolds for droplet
927 formation and positioning in several membraneless organelles [29], and thus coiled-coil
928 containing proteins could play a role in pyrenoid nucleation.

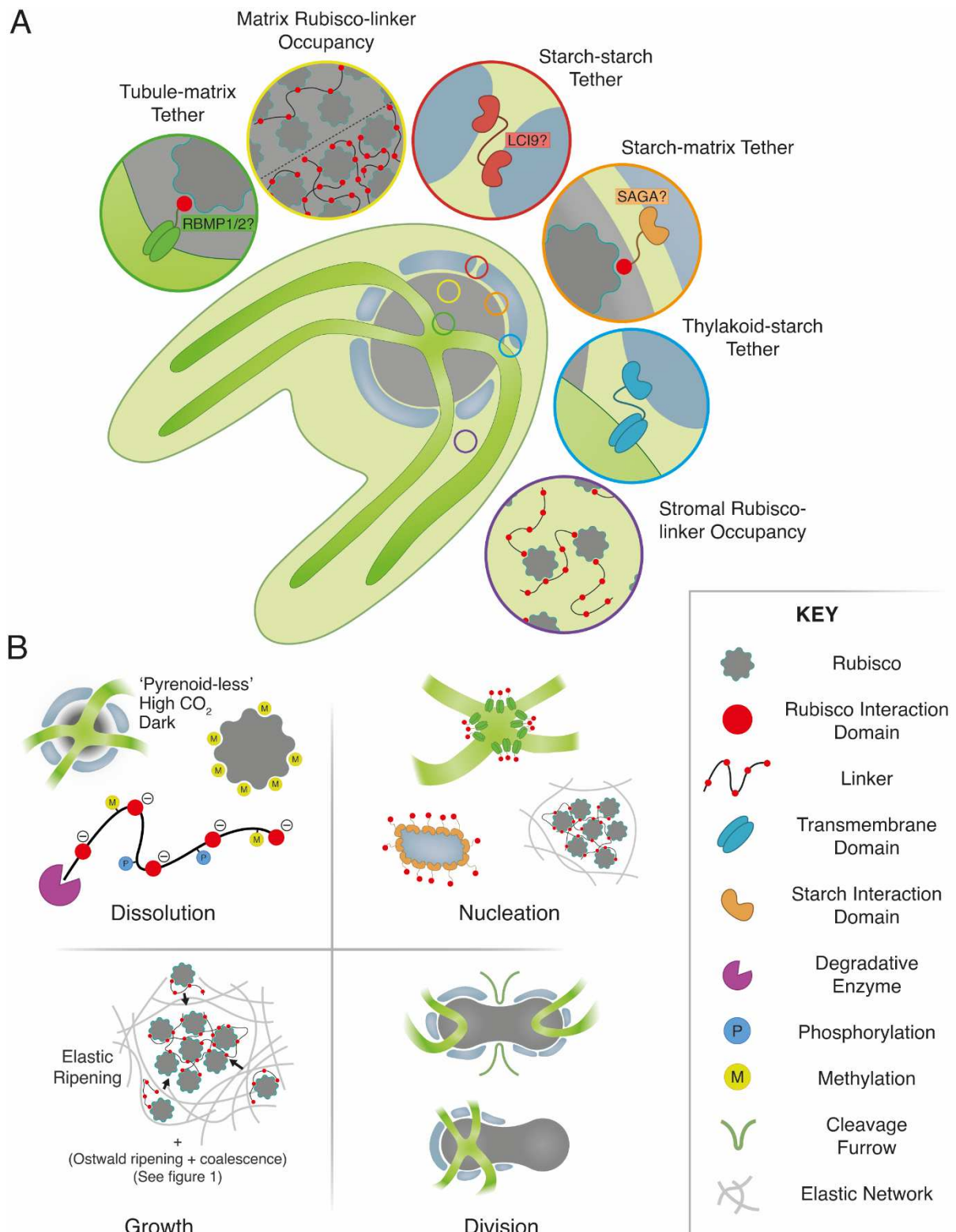
929 Subsequent growth of the canonically positioned matrix is unexplored, but has multiple
930 potential explanations based on descriptions of other biological condensates. If the droplet
931 nucleated at the canonical position has a larger droplet size, due to pre-seeding or
932 concentration-dependent effects, Ostwald ripening would preferentially drive the growth of this
933 droplet (Figure 1) [224]. Similarly, growth could be driven by elastic ripening, in which the
934 transport of solute down a stiffness gradient results in the preferential growth of droplets at
935 areas of low stiffness, on a faster timescale than Ostwald ripening [26, 225] (Figure 5B).
936 Mechanical heterogeneity within the *Chlamydomonas* chloroplast has not been characterised,

937 but it is possible the absence of thylakoid stacks at the canonical position contributes reduced
938 network stiffness and facilitates a stiffness gradient [226].

939 *De novo* formation of multiple proto-pyrenoid puncta in the stroma of daughter cells
940 suggests nucleation also occurs separate to the canonical pyrenoid position. It is possible that
941 fluctuations in local concentrations of EPYC1 and Rubisco could provide a basis for nucleation,
942 independent of structural features that contribute seeding effects. Additionally, given the rapid
943 timescale for nucleation and re-condensation following division (<1 hour), it is likely the same
944 PTM control mechanisms important for dissolution are also poignant here. Similarly, light-
945 induced re-condensation occurs during an ~4 hour window [194], with low CO₂-induced
946 reformation occurring over similarly longer timescales [193], suggesting alternate mechanisms
947 for controlled nucleation in these instances.

948

949



950
951
952
953
954
955
956
957
958

Figure 5. Key unanswered questions in the *Chlamydomonas pyrenoid*. **A)** Molecular basis for pyrenoid localization at key ultrastructural features (clockwise from top left). A predicted pyrenoid tubule-enriched Rubisco-binding protein that could contribute to canonical positioning and localization of the pyrenoid matrix, as in B, perhaps contributed by RBMP1/2. The unknown occupancy of the Rubisco-linker interaction that underpins LLPS of the matrix, where the dashed line demarcates a low Rubisco, high linker occupancy and a high Rubisco, low linker occupancy scenario. A putative protein interaction that spans the inter-starch gaps in the sheath to tether

959 adjacent plates, possibly fulfilled by LCI9, as highlighted in Mackinder et al, [80]. A starch-
960 associated Rubisco-interacting protein that tethers the starch sheath to the matrix, possibly
961 underpinning an alternative starch-centric nucleation model, as in B, perhaps performed by
962 SAGA1/2 [42] among others. A putative thylakoid-associated, starch-binding protein that could
963 explain the canonical positioning of the starch plates in pyrenoid-less strains. The uncharacterized
964 occupancy and oligomeric state of the Rubisco-linker interaction in the dilute stromal phase. **B)**
965 Potential control mechanisms underpinning the dynamics of the pyrenoid. Dissolution, clockwise
966 from top left. The dissolved state of the pyrenoid, showing canonical positioning of the starch plates
967 and retention of a portion of the matrix at the tubule intersection, possibly forming an
968 interdependent assembly point. A methylated state of Rubisco that could disrupt linker interactions
969 and contribute to dissolution. Potential linker perturbations that could contribute to phase
970 transitions, including PTMs (phosphorylation and methylation) as well as degradation
971 (concentration effect) and charge perturbation (pH and ion concentration). Nucleation, from top left.
972 Tubule-enriched matrix tethers, that could nucleate a canonically positioned pyrenoid, consistent
973 with A. Spontaneous nucleation at a region of low elastic density in the stroma. Starch-centric
974 nucleation, seeded by starch-matrix tethers, consistent with A. Growth, multiple explanations for
975 pyrenoid growth following *de novo* formation. Division, possibilities for ultrastructural distribution
976 through cleavage furrow-induced pyrenoid fission.

977
978
979

980 **DOES LLPS UNDERPIN PYRENOID ASSEMBLY ACROSS LINEAGES?**

981 Pyrenoids in all lineages consist of an electron-dense matrix that is believed to be a Rubisco
982 condensate. This assumption is based on observations across pyrenoid containing lineages
983 that the pyrenoid matrix contains most of the cell's Rubisco [55, 70, 71, 88, 133, 140, 217,
984 227-232]. To date there is only conclusive evidence in *Chlamydomonas* that the pyrenoid is a
985 LLPS organelle [36, 44], however there are several lines of evidence that suggest that
986 pyrenoids are LLPS across diverse lineages. Pyrenoids normally have spherical/elliptical
987 shapes, which is typical for organelles formed by LLPS and not bound by membranes, given
988 their surface tension effects. As outlined above, the observation of pyrenoid division via fission
989 and examples of *de novo* assembly and apparent Ostwald ripening also supports the idea that
990 LLPS is a general property of all pyrenoids. In addition, dissolution of the pyrenoid and dynamic
991 Rubisco relocalization has been reported across diverse algae including the dinoflagellate
992 *Gonyaulax* [233] and the green alga *Dunaliella tertiolecta* [234] and *Euglena gracilis* [133].

993 Along with observational evidence, bioinformatic analysis revealed the occurrence of
994 proteins in a broad range of algae that show similarities to the *Chlamydomonas* Rubisco linker
995 protein EPYC1 [51]. These proteins have a similar repeat number, length, isoelectric point and
996 disorder profile to EPYC1 indicating a putative function as linker proteins. All in all, the
997 observed spherical shape of the pyrenoid, the observation of pyrenoid fission and identification
998 of proposed Rubisco linker proteins, suggests that pyrenoids are formed by LLPS across algal
999 lineages. However, essential experimental evidence to support pyrenoid LLPS in diverse algae
1000 is missing.

1001
1002

1002 **PYRENOID EVOLUTION**

1003 Even though pyrenoids occur in all algal lineages and in hornworts, not all algae or hornwort
1004 species contain pyrenoids. Pyrenoid-less algae (e.g. the extremophile rhodophyte class
1005 *Cyanidiophyceae*, members of the chlorophyte genera *Bathycoccus* and *Chloromonas*, the
1006 TSAR class chrysophyte (golden algae), and most species of the eustigmatophyte genus
1007 *Nannochloropsis*) and hornworts that lack pyrenoids are spotted across the phylogenetic tree,

1008 suggesting that pyrenoids were lost and gained multiple times during evolution [50, 235, 236],
1009 possibly with hundreds of evolutionary origins [15]. The exact distribution of pyrenoids is
1010 unknown since the anatomy of many algae has never been investigated thoroughly. Moreover,
1011 the occurrence of a pyrenoid in different algal species could depend on factors such as CO₂
1012 abundance, light and life-cycle stage. Thus, the apparent absence of pyrenoids in some
1013 species might be attributed to the metabolic state of the imaged cells, life-cycle stage or even
1014 missed due to insufficient imaging.

1015 The evolutionary history of the pyrenoid is complex and presently poorly understood.
1016 Our best understanding of pyrenoid evolution comes from hornworts where pyrenoids have
1017 evolved at least 5-6 times independently and have also been lost at least 5-6 times [50]. The
1018 first hornwort pyrenoids appeared ~100 million years ago, a time that coincided with a drastic
1019 decline of atmospheric CO₂ levels. However, other younger pyrenoid-containing clades
1020 originated during periods with higher atmospheric CO₂ levels and pyrenoids were apparently
1021 lost in hornwort clades during periods with relatively low atmospheric CO₂ levels [50]. Taken
1022 together, these findings suggest that pyrenoids in hornworts did not evolve solely as a
1023 response to atmospheric CO₂ levels but must also offer further evolutionary advantages.
1024 Hornworts are typically found in terrestrial habitats growing on soil banks or epiphytic on trees
1025 and leaves but can also be semiaquatic growing partially submerged or undergoing temporal
1026 submersion in freshwater habitats [237]. In algae, the evolution of pyrenoids and a biophysical
1027 CCM is widely considered as an adaptation to their aquatic lifestyles, where HCO₃⁻ is more
1028 abundant than CO₂ and the CO₂ diffusion to Rubisco is limited [238]. However, this adaptation
1029 to aquatic environments is not clear in hornworts, with some semiaquatic hornwort species
1030 lacking pyrenoids, whereas several terrestrial hornwort species contain pyrenoids [237].

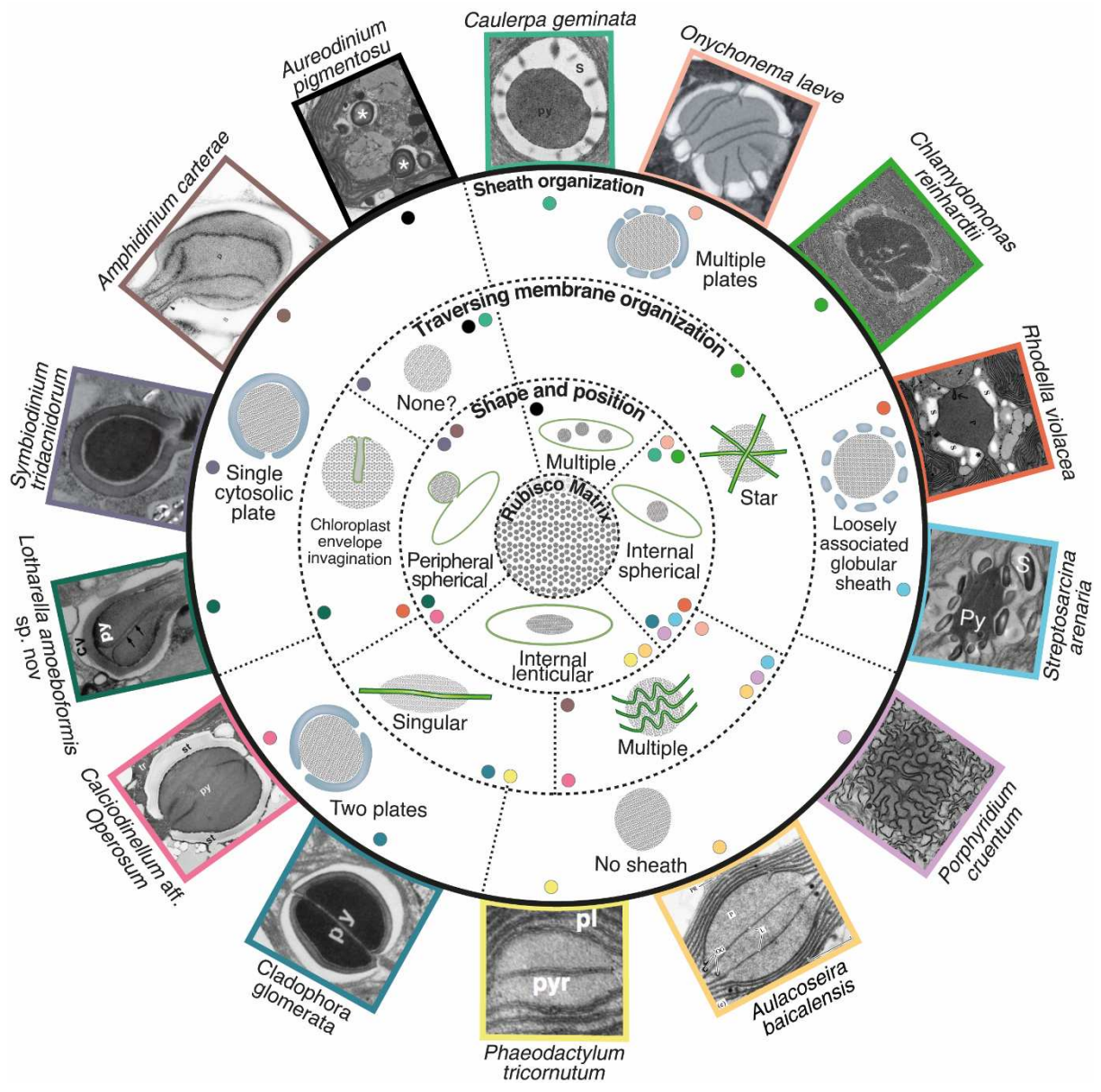
1031 It has been proposed that the lack of pyrenoids in all other land plants indicates that
1032 the last common ancestor of all hornworts had no pyrenoid and that pyrenoids in hornworts
1033 evolved independently of ancestral algal pyrenoids [50]. However, recent genomic data is
1034 offering some new insights into pyrenoid evolution [239]. Some pyrenoid localized core green
1035 algal CCM components, like LCIB and CAH3, appear to have homologs in hornworts (but not
1036 land plants), while others, like EPYC1 or RBMP1/2, have no homologs (although sequence
1037 divergence may be accelerated for intrinsically disordered proteins). This suggests that the
1038 common ancestor of green algae and hornworts (and hence land plants) may have had a
1039 biophysical CCM. With biophysical CCM loss at both a genetic and functional level occurring
1040 in land plants but retained in hornworts (at least at a genetic level) with the then subsequent
1041 loss or replacement of individual components during pyrenoid and CCM loss and re-acquisition
1042 during hornwort evolution. The identification of analogous pyrenoid components across
1043 lineages will likely shed some light on pyrenoid evolution.

1044

1045 **Pyrenoid structural diversity across different algal lineages**

1046 Pyrenoid structure varies greatly between different algal and hornwort species (Figure 6).
1047 Common to all pyrenoids is that they consist of a dense Rubisco matrix, which is probably
1048 formed through LLPS (see discussion above). Variation in matrix staining across species
1049 suggests differences in matrix protein concentration but could also be due to fixation artefacts
1050 and differences in fixation protocols. Of note, found within the matrix of some hornwort and all
1051 *Trebouxia* (chlorophyta) lichen symbionts are lipid-rich globules called pyrenoglobuli [140,
1052 240]. Whereas most species have only one pyrenoid per chloroplast, some species have two
1053 or more [23, 170, 241, 242], sometimes even ultrastructurally distinct pyrenoids [243]. In the
1054 chlorophyte *Spirogyra*, each chloroplast has multiple evenly-sized pyrenoids [23, 242],
1055 suggesting that Rubisco condensation is controlled by an unknown mechanism, which

1056 prevents Ostwald ripening and thus allows the coexistence of multiple pyrenoids instead of
1057 fusing into one as observed in *Chlamydomonas* [36, 44]. In many species the pyrenoid is
1058 localized centrally in the chloroplast amidst the thylakoids (common in glaucophytes and all
1059 green lineages; some rhodophytes and diatoms), in other species the pyrenoid is localized in
1060 peripheral protrusions of the chloroplast (common in all TSAR lineages and some
1061 rhodophytes). In species with a peripheral pyrenoid the pyrenoid is tightly encircled by the
1062 chloroplast envelope and the protrusion is typically into the central cytosolic space. In many
1063 species the pyrenoid is traversed by one or more membrane tubules that typically are
1064 continuous with the thylakoid membrane (for clarity, in the following we term these thylakoid
1065 tubules) but can be derived from other cellular membranes, collectively these are termed
1066 pyrenoid tubules. The thylakoid tubules are presumably important for the delivery of inorganic
1067 carbon as discussed above for *Chlamydomonas* and postulated in the diatom *Phaeodactylum*
1068 *tricornutum*, whose single pyrenoid tubule contains a carbonic anhydrase [244]. Observations
1069 across lineages indicate that thylakoid tubules are biochemically distinct from other parts of
1070 the thylakoid membrane. Thylakoid tubules across lineages typically lack active PSII, which
1071 would produce O₂ in close proximity to Rubisco and thus promote the oxygenase function of
1072 Rubisco, reducing photosynthetic performance [55, 88, 117, 118].
1073



1074
 1075
 1076
 1077
 1078
 1079
 1080
 1081
 1082
 1083
 1084
 1085
 1086
 1087
 1088
 1089
 1090
 1091
 1092

Figure 6. Pyrenoids are structurally diverse. Peripheral TEM images are used to demonstrate non-exhaustive examples of combinations of pyrenoid structural features. Starting centrally, with the defining pyrenoid matrix and radiating outwards, combinations of matrix shape/position, traversing membrane organization and sheath organization can be achieved. Observed combinations are loosely demarcated by dashed lines between and within rings, but no combinations are definitively excluded. Coloured dots indicate combinations of structural features, corresponding to image borders. Image labelling is from original publication: p/py/pyr/*, pyrenoid; s/st, starch; pl, plastid; cv, capping vesicle. References for images, clockwise from *Caulerpa geminata* [245], *Onychonema laeve* [100], *Chlamydomonas reinhardtii* (authors collection), *Rhodella violacea* [246], *Streptosarcina arenaria* [247], *Porphyridium cruentum* [55], *Aulacoseira baicalensis* [248], *Phaeodactylum tricornutum* [249], *Cladophora glomerata* [250], *Calciadinellum aff. Operosum* [60], *Lotharella amoebiformis* sp. nov [251], *Symbiodinium tridacnidorum* [252], *Amphidinium carterae* [148], *Aureodinium pigmentosum* [253].

Although it is currently assumed that the thylakoid tubules are important for the delivery of inorganic carbon to the pyrenoid, not all pyrenoid containing species have a matrix traversed

1093 by thylakoid tubules. Thylakoid tubules are seen in all hornwort pyrenoids and there are
1094 example species in all algal lineages except for glaucophytes. With data in many species
1095 limited to a handful of TEM images, it is possible that TEM sectioning could fail to reveal
1096 tubules. In species with peripheral pyrenoids the thylakoid tubules are often missing. In these
1097 species, the thylakoid membrane often stops before the pyrenoid matrix begins [131, 246, 254,
1098 255] and, in some cases, the thylakoid tips extend into the matrix [256]. However, there are
1099 exceptions (e.g. dinophytes), where thylakoid tubules cross the matrix of peripheral pyrenoids
1100 completely or even form networks in them [60, 257]. In species with peripheral pyrenoids
1101 without thylakoid tubules, the chloroplast envelope can extend into the pyrenoid matrix by
1102 forming tubular intrusions, indicating that membranes traversing the pyrenoid is potentially a
1103 ubiquitous feature. In striking examples of such envelope intrusions, the internal region of the
1104 pyrenoid seems to be directly connected to the cytosol, nucleus or mitochondria. The nuclear
1105 envelope of the rhodophyte *Rhodella violacea* is in direct contact with the chloroplast and
1106 elongation of the nuclear envelope into the pyrenoid at a chloroplast envelope intrusion
1107 suggests interaction between the nucleus and the pyrenoid [246]. In the chlorophyte
1108 *Prasinoderma singularis* it is claimed that the mitochondria protrudes through the chloroplast
1109 envelope intrusion into the pyrenoid [258], opening the possibility that photorespiratory CO₂
1110 release could directly be driving photosynthetic carbon fixation. The function of all pyrenoid
1111 traversing chloroplast envelope intrusions remain unknown, but it seems likely that they are
1112 also involved in CO₂ delivery to the pyrenoid.

1113 The characteristics and complexity of pyrenoid tubules varies greatly between species
1114 (Figure 6). Tubules have been used as taxonomic markers in some lineages (e.g. in
1115 dinophytes [259] or diatoms [248]). The least complex examples are where the pyrenoid is
1116 traversed only by a single thylakoid tubule, which is found in some chlorophytes and diatoms
1117 [248, 260, 261]. In several chlorophyte, dinophyte and euglenophyte species the pyrenoid is
1118 traversed by multiple non-connecting parallel membranes [248, 261-263]. Other species form
1119 more or less complex, interconnected thylakoid tubule networks within the pyrenoid matrix,
1120 which is common in chlorophyte, rhodophyte and hornwort species. Some species like
1121 *Chlamydomonas* have relatively simple star-shaped (2D view or stellate as seen in 3D)
1122 thylakoid tubule networks crossing their pyrenoid, whilst other species like the rhodophyte
1123 *Porphyridium cruentum* [127, 129], the chlorophyte genus *Zygnema* [264-266] or hornworts
1124 [50] show highly complex networks of interconnected tubules. The thylakoid tubules can
1125 drastically differ from the rest of the thylakoid network as stacked membranes usually unstack
1126 and enter the pyrenoid as single entities or merge and enter the pyrenoid as composites.
1127 However, in other species the thylakoid membrane appears not to change as it enters the
1128 pyrenoid matrix, for instance the hornwort genus *Dendroceros* maintains even grana stacks in
1129 the pyrenoid matrix [50].

1130 Even though different algal lineages use different carbohydrates for energy storage,
1131 there are example species from all algal clades that surround their pyrenoid with a layer of
1132 their storage material (hereafter referred to as starch sheath). This is even more astonishing
1133 considering that rhodophytes and algal lineages that inherited a “red” chloroplast through
1134 secondary endosymbiosis store their reserve material not in the chloroplast but in the cytosol.
1135 Consequently, only peripheral pyrenoids in “red” chloroplasts exhibit a starch sheath and
1136 central pyrenoids are always sheath-less in these lineages. Glaucophytes never have a starch
1137 sheath, and in the green lineages the pyrenoid is often, but not always, surrounded by a starch
1138 sheath. The morphology of the starch sheath varies greatly between species (Figure 6). The
1139 starch sheath can be formed by only one plate [254, 267, 268] and in species, where the
1140 pyrenoid matrix is crossed by a single thylakoid disc, the starch sheath is sometimes formed

1141 by two plates [250, 269], but in most cases the starch sheath is formed by several plates. In
1142 some species there are broad gaps between the starch plates [62, 246, 247], whereas in
1143 others the plates sit tightly together, sometimes even in multiple layers [270]. The starch
1144 sheath has been posited to function as a structural barrier that prevents CO₂ leakage from the
1145 pyrenoid, with some supporting evidence for this in *Chlamydomonas* [42, 73, 91].

1146 Differences in pyrenoid structure across algae indicates that inorganic carbon flow from
1147 the external environment to Rubisco must differ from the described mechanism for
1148 *Chlamydomonas*. In species with pyrenoids lacking thylakoid tubules, inorganic carbon must
1149 enter the pyrenoid matrix directly from the chloroplast stroma without entering the thylakoid
1150 lumen or even from the cytosol in the case of peripheral pyrenoids without even entering the
1151 chloroplast stroma, perhaps through chloroplast envelope intrusions that extend into the
1152 pyrenoid matrix. Species without a starch sheath around the pyrenoid potentially lose more
1153 CO₂ through leaking than species with a starch sheath. However, the presence of low electron
1154 dense CO₂ impermeable protein layers or membrane diffusion barriers created from adjacent
1155 thylakoids or the chloroplast envelope cannot be ruled out.

1156 Outside of *Chlamydomonas*, we currently lack a molecular understanding of the
1157 structural arrangement of the pyrenoid across algal lineages and hornworts) and,
1158 consequently, mostly understand the operation of these CCMs by analogy to
1159 *Chlamydomonas*. Thus, it will be key to obtain information on the structure and function of
1160 pyrenoids from other algae as well as from hornworts in order to fully understand the principles
1161 of CCM function, which is pivotal for any engineering approaches into crop plants. Moreover,
1162 a deeper knowledge of the pyrenoid structure and function of ecologically relevant algae, such
1163 as diatoms and coccolithophores, will help to better understand global carbon flows.

1164

1165 **SYNTHETIC PYRENOID ASSEMBLY AND RELEVANCE TO HIGHER PLANT** 1166 **ENGINEERING**

1167

1168 In modern agriculture where biotic and abiotic stresses such as water and nitrogen availability,
1169 pests and pathogens can be controlled, crop yield can become limited by CO₂ fixation by
1170 photosynthesis [271]. Calculations show that many C₃ crops, such as rice, wheat and soya are
1171 only reaching at maximum one-third of their theoretical potential of conversion of solar energy
1172 capture to carbohydrate synthesis [272]. It is thought that photosynthetic performance has not
1173 been selected for through breeding programmes due to it being highly conserved within crop
1174 species giving very little room for positive selection [17]. A promising strategy for
1175 photosynthetic improvements is the engineering of a CCM (see [201, 273-275] for recent
1176 detailed reviews). Modelling has shown that biophysical CCM engineering in the form of a
1177 pyrenoid or carboxysome centred CCM could result in theoretical yield increases of 60% along
1178 with improvements in water and nitrogen use efficiencies [17, 276]. However, predicting yield
1179 increases from photosynthetic improvements is complicated due to the complex interplay of
1180 multiple processes that determine crop yield. This has been demonstrated by cross-scale
1181 modelling that indicate that simultaneous improvements in Rubisco activity (i.e. CCM
1182 presence), electron transport and mesophyll conductance maybe required for significant yield
1183 improvements [277]. Field data in tobacco supports photosynthetic engineering as a promising
1184 approach with significant increases in plant biomass seen with multiple approaches, including
1185 synthetic photorespiratory bypasses to reduce photorespiration [278], enhanced
1186 photoprotection [279] and combined improvements in RuBP regeneration and electron
1187 transport [280]. Although, how biomass improvements will translate to grain crop yields is
1188 unclear. The potential for increasing CO₂ supply to Rubisco through CCM engineering to

1189 translate into grain yield improvements is supported to some extent by in field data where
1190 season-long CO₂ enrichment using free-air concentration enrichment (FACE) technology has
1191 demonstrated yield improvements on average of 17% across rice, wheat, cotton and sorghum
1192 [271].

1193 Algal CCM engineering is currently underway with successful expression of multiple
1194 CCM components that correctly localize in Arabidopsis [281]. To prime plants for pyrenoid
1195 assembly via EPYC1, Arabidopsis lines that have had the majority of their native Rubisco SSU
1196 replaced with *Chlamydomonas* Rubisco SSU have been developed and the hybrid Rubisco
1197 shown to be functional [282]. Purified Arabidopsis/ *Chlamydomonas* hybrid Rubisco has then
1198 been shown to undergo LLPS *in vitro* [97]. Optimised EPYC1 expression in Arabidopsis
1199 expressing *Chlamydomonas* Rubisco SSU has recently resulted in *in planta* proto-pyrenoid
1200 assembly (i.e. EPYC1/ Rubisco condensation) [283], with Arabidopsis proto-pyrenoids having
1201 a comparable size and internal mixing to *Chlamydomonas* pyrenoids [36, 283]. In contrast to
1202 *in planta* carboxysome assembly where Rubisco packaging results in severely reduced plant
1203 growth [284], proto-pyrenoid expressing lines have a similar photosynthetic performance to
1204 wild-type [283]. Although plant proto-pyrenoid assembly is a major breakthrough,
1205 photosynthetic improvements most likely will only be realized once a complete CCM is
1206 assembled. Based on conserved structural features of pyrenoids across algae and our current
1207 knowledge of the CCM, a minimum CCM is expected to require: 1) Rubisco/EPYC1 matrix
1208 assembly around thylakoids; 2) inorganic carbon delivery to the matrix traversing thylakoids
1209 via HCO₃⁻ channels; and 3) accelerated dehydration of HCO₃⁻ to CO₂ via a carbonic anhydrase
1210 localized in the matrix traversing thylakoids. Further pyrenoid structural refinements may
1211 include modification of thylakoids traversing the pyrenoid matrix, similar to pyrenoid tubule
1212 assemblies observed in *Chlamydomonas*; the assembly of a pyrenoid starch sheath to
1213 minimise CO₂ retro diffusion out of the pyrenoid; and additional inorganic carbon accumulation
1214 systems at the chloroplast envelope (i.e. LCIA) and the pyrenoid periphery (i.e. LCIB/LCIC
1215 complex). In addition, detailed understanding and engineering control of pyrenoid assembly,
1216 regulation and division within different plant leaf cell-types will be critical for successful
1217 function. Understanding pyrenoid assembly across diverse algae will offer additional
1218 approaches to engineering plants with pyrenoid CCMs. Moreover, it will also open
1219 opportunities for hybrid assemblies and the development of synthetic/designer parts. A primary
1220 example could be the development of synthetic EPYC1 analogues that can phase separate
1221 plant Rubisco removing the requirement to modify plant Rubisco SSU.

1222

1223

1224 **SUMMARY**

1225

1226 The pyrenoid is a biogeochemically important organelle central to biophysical CCMs that
1227 contribute massively to photosynthetic primary production and offer serious prospect for
1228 enhancing crop yields. Once considered amorphous/crystalline, recent work has allowed
1229 characterization of the *Chlamydomonas* pyrenoid as a LLPS body, formed by complex
1230 coacervation between Rubisco and a disordered linker protein, EPYC1. The liquid-like
1231 properties of the pyrenoid play a critical role in ensuring robust pyrenoid inheritance and most
1232 likely enable rapid adaption of carbon fixation through the CBB cycle in response to changes
1233 in inorganic carbon and light availability. The commonality of pyrenoid dynamics,
1234 ultrastructural features and putative Rubisco linkers described across the eukaryotic tree of
1235 life suggest that LLPS may be common to the functionality of pyrenoids, however conclusive
1236 evidence across diverse phyla is currently lacking. Despite rapid recent advances in our

1237 understanding of the *Chlamydomonas* pyrenoid as a LLPS organelle, key gaps in our
1238 knowledge exist. We are only beginning to understand the basis of the molecular structure that
1239 underpins the defining macroscopic properties and ultrastructural arrangements exhibited by
1240 pyrenoids. Understanding the molecular basis for phase separation will facilitate an
1241 understanding of the processes that determine the dynamic transitions of the pyrenoid, most
1242 likely essential to its adaptive function across lineages. Additionally, understanding the role of
1243 ultrastructural features and their associated molecular factors in pyrenoid assembly,
1244 localization and division will be central to understanding the underlying properties for pyrenoid
1245 function. This understanding will have direct implications for the rapidly evolving efforts to
1246 introduce pyrenoids into higher plants, that have been somewhat retarded by key gaps in our
1247 knowledge. From a molecular scale to global impact, extending our in-depth knowledge of
1248 pyrenoid function to diverse and globally important pyrenoid-containing lineages will facilitate
1249 our understanding of how/if Rubisco LLPS has driven the complex evolutionary history of the
1250 pyrenoid and provide molecular level biophysical based principles that underly ~30% of global
1251 carbon fixation.

1252

1253 **ACKNOWLEDGEMENTS**

1254 We would like to thank the support and constructive comments from Avi Flamholz, Moritz
1255 Meyer, Ursula Goodenough, Martin Jonikas, Alistair McCormick, Nicky Atkinson, Liat Adler,
1256 Aranzazú Díaz Ramos, Charlotte Walker and Eleanor Fletcher whose input dramatically
1257 improved the review. The review was supported by funding from UK Biotechnology and
1258 Biological Sciences Research Council (BBSRC) Grants BB/R001014/1 and BB/S015337/1 (to
1259 LCMM); Leverhulme Trust Grant RPG-2017-402 (to LCMM); UK Research and Innovation
1260 Future Leader Fellowship MR/T020679/1 (to LCMM) and BBSRC DTP2 BB/M011151/1a (to
1261 JB and LCMM).

1262

1263 **REFERENCES**

1264

- 1265 [1] C.B. Field, M.J. Behrenfeld, J.T. Randerson, P. Falkowski, Primary production of the
1266 biosphere: integrating terrestrial and oceanic components, *Science*, 281 (1998) 237-240.
1267 [2] A. Bar-Even, E. Noor, Y. Savir, W. Liebermeister, D. Davidi, D.S. Tawfik, R. Milo, The
1268 Moderately Efficient Enzyme: Evolutionary and Physicochemical Trends Shaping Enzyme
1269 Parameters, *Biochemistry*, 50 (2011) 4402-4410.
1270 [3] S.M. Whitney, R.L. Houtz, H. Alonso, Advancing our understanding and capacity to
1271 engineer nature's CO₂-sequestering enzyme, Rubisco, *Plant Physiol.*, 155 (2011) 27-35.
1272 [4] G.G.B. Tcherkez, G.D. Farquhar, T.J. Andrews, Despite slow catalysis and confused
1273 substrate specificity, all ribulose biphosphate carboxylases may be nearly perfectly
1274 optimized, *Proceedings of the National Academy of Sciences*, 103 (2006) 7246-7251.
1275 [5] R.A. Studer, P.-A. Christin, M.A. Williams, C.A. Orengo, Stability-activity tradeoffs
1276 constrain the adaptive evolution of RubisCO, *Proceedings of the National Academy of
1277 Sciences*, 111 (2014) 2223-2228.
1278 [6] A.I. Flamholz, N. Prywes, U. Moran, D. Davidi, Y.M. Bar-On, L.M. Oltrogge, R. Alves, D.
1279 Savage, R. Milo, Revisiting Trade-offs between Rubisco Kinetic Parameters, *Biochemistry*,
1280 58 (2019) 3365-3376.
1281 [7] J. Galmés, M.V. Kapralov, P.J. Andralojc, M.À. Conesa, A.J. Keys, M.A.J. Parry, J.
1282 Flexas, Expanding knowledge of the Rubisco kinetics variability in plant species:
1283 environmental and evolutionary trends, *Plant, Cell & Environment*, 37 (2014) 1989-2001.
1284 [8] R.J. Ellis, The most abundant protein in the world, *Trends Biochem. Sci.*, 4 (1979) 241-
1285 244.

1286 [9] J.A. Raven, Rubisco: still the most abundant protein of Earth?, *New Phytol.*, 198 (2013) 1-
1287 3.

1288 [10] G.D. Price, M.R. Badger, Expression of Human Carbonic Anhydrase in the
1289 Cyanobacterium *Synechococcus* PCC7942 Creates a High CO₂-Requiring Phenotype
1290 Evidence for a Central Role for Carboxysomes in the CO₂ Concentrating Mechanism, *Plant*
1291 *Physiol.*, 91 (1989) 505-513.

1292 [11] J. Karlsson, A.K. Clarke, Z.Y. Chen, S.Y. Huggins, Y.I. Park, H.D. Husic, J.V. Moroney,
1293 G. Samuelsson, A novel alpha-type carbonic anhydrase associated with the thylakoid
1294 membrane in *Chlamydomonas reinhardtii* is required for growth at ambient CO₂, *EMBO J.*,
1295 17 (1998) 1208-1216.

1296 [12] N.M. Mangan, A. Flamholz, R.D. Hood, R. Milo, D.F. Savage, pH determines the
1297 energetic efficiency of the cyanobacterial CO₂ concentrating mechanism, *Proc. Natl. Acad.*
1298 *Sci. U. S. A.*, 113 (2016) E5354-5362.

1299 [13] A. Flamholz, P.M. Shih, Cell biology of photosynthesis over geologic time, *Current*
1300 *Biology*, 30 (2020) R490-R494.

1301 [14] B.D. Rae, B.M. Long, M.R. Badger, G.D. Price, Functions, compositions, and evolution
1302 of the two types of carboxysomes: polyhedral microcompartments that facilitate CO₂ fixation
1303 in cyanobacteria and some proteobacteria, *Microbiol. Mol. Biol. Rev.*, 77 (2013) 357-379.

1304 [15] M.T. Meyer, M.M.M. Goudet, H. Griffiths, The Algal Pyrenoid, in: A.W.D. Larkum, A.R.
1305 Grossmann, J.A. Raven (Eds.) *Photosynthesis in Algae: Biochemical and Physiological*
1306 *Mechanisms*, Springer International Publishing, Place Published, 2020, pp. 179-203.

1307 [16] J.A. Raven, The possible roles of algae in restricting the increase in atmospheric CO₂
1308 and global temperature, *Eur. J. Phycol.*, 52 (2017) 506-522.

1309 [17] S.P. Long, S. Burgess, I. Causton, Redesigning crop photosynthesis, in: R. Zeigler (Ed.)
1310 *Sustaining Global Food Security: The Nexus of Science and Policy*, CSIRO Publishing,
1311 Place Published, 2019, pp. 128-147.

1312 [18] D.K. Ray, N.D. Mueller, P.C. West, J.A. Foley, Yield trends are insufficient to double
1313 global crop production by 2050, *PLoS One*, 8 (2013) e66428.

1314 [19] S. Alberti, Phase separation in biology, *Curr. Biol.*, 27 (2017) R1097-R1102.

1315 [20] S. Boeynaems, S. Alberti, N.L. Fawzi, T. Mittag, M. Polymenidou, F. Rousseau, J.
1316 Schymkowitz, J. Shorter, B. Wolozin, L. Van Den Bosch, P. Tompa, M. Fuxreiter, Protein
1317 Phase Separation: A New Phase in Cell Biology, *Trends Cell Biol.*, 28 (2018) 420-435.

1318 [21] P. Li, S. Banjade, H.-C. Cheng, S. Kim, B. Chen, L. Guo, M. Llaguno, J.V. Hollingsworth,
1319 D.S. King, S.F. Banani, P.S. Russo, Q.-X. Jiang, B.T. Nixon, M.K. Rosen, Phase transitions
1320 in the assembly of multivalent signalling proteins, *Nature*, 483 (2012) 336-340.

1321 [22] S.F. Banani, H.O. Lee, A.A. Hyman, M.K. Rosen, Biomolecular condensates: organizers
1322 of cellular biochemistry, *Nat. Rev. Mol. Cell Biol.*, 18 (2017) 285-298.

1323 [23] J.-P. Vaucher, *Histoire des conferves d'eau douce, contenant leurs différens modes de*
1324 *reproduction, et la description de leurs principales espèces, suivie de l'histoire des trémelles*
1325 *et des ulves d'eau douce. Par Jean-Pierre Vaucher, Place Published, 1803.*

1326 [24] C.P. Brangwynne, C.R. Eckmann, D.S. Courson, A. Rybarska, C. Hoegel, J. Gharakhani,
1327 F. Jülicher, A.A. Hyman, Germline P granules are liquid droplets that localize by controlled
1328 dissolution/condensation, *Science*, 324 (2009) 1729-1732.

1329 [25] A.A. Hyman, C.A. Weber, F. Jülicher, Liquid-liquid phase separation in biology, *Annu.*
1330 *Rev. Cell Dev. Biol.*, 30 (2014) 39-58.

1331 [26] K.A. Rosowski, T. Sai, E. Vidal-Henriquez, D. Zwicker, R.W. Style, E.R. Dufresne,
1332 Elastic ripening and inhibition of liquid-liquid phase separation, *Nat. Phys.*, 16 (2020) 422-
1333 425.

1334 [27] D.T. McSwiggen, M. Mir, X. Darzacq, R. Tjian, Evaluating phase separation in live cells:
1335 diagnosis, caveats, and functional consequences, *Genes Dev.*, 33 (2019) 1619-1634.

1336 [28] C.L. Cuevas-Velazquez, J.R. Dinneny, Organization out of disorder: liquid-liquid phase
1337 separation in plants, *Curr. Opin. Plant Biol.*, 45 (2018) 68-74.

1338 [29] D.M. Mitrea, R.W. Kriwacki, Phase separation in biology; functional organization of a
1339 higher order, *Cell Commun. Signal.*, 14 (2016) 1.

1340 [30] G.L. Dignon, R.B. Best, J. Mittal, Biomolecular Phase Separation: From Molecular
1341 Driving Forces to Macroscopic Properties, *Annu. Rev. Phys. Chem.*, 71 (2020) 53-75.

1342 [31] I. Peran, T. Mittag, Molecular structure in biomolecular condensates, *Curr. Opin. Struct.*
1343 *Biol.*, 60 (2020) 17-26.

1344 [32] J.-M. Choi, R.V. Pappu, The Stickers and Spacers Framework for Describing Phase
1345 Behavior of Multivalent Intrinsically Disordered Proteins, *Biophys. J.*, 118 (2020) 492a.

1346 [33] J.-M. Choi, A.S. Holehouse, R.V. Pappu, Physical Principles Underlying the Complex
1347 Biology of Intracellular Phase Transitions, *Annu. Rev. Biophys.*, 49 (2020) 107-133.

1348 [34] S.F. Banani, A.M. Rice, W.B. Peeples, Y. Lin, S. Jain, R. Parker, M.K. Rosen,
1349 Compositional Control of Phase-Separated Cellular Bodies, *Cell*, 166 (2016) 651-663.

1350 [35] I. Owen, F. Shewmaker, The Role of Post-Translational Modifications in the Phase
1351 Transitions of Intrinsically Disordered Proteins, *Int. J. Mol. Sci.*, 20 (2019) 5501.

1352 [36] E.S. Freeman Rosenzweig, B. Xu, L. Kuhn Cuellar, A. Martinez-Sanchez, M. Schaffer,
1353 M. Strauss, H.N. Cartwright, P. Ronceray, J.M. Plitzko, F. Förster, N.S. Wingreen, B.D.
1354 Engel, L.C.M. Mackinder, M.C. Jonikas, The Eukaryotic CO₂-Concentrating Organelle Is
1355 Liquid-like and Exhibits Dynamic Reorganization, *Cell*, 171 (2017) 148-162.e119.

1356 [37] M. Feric, C.P. Brangwynne, A nuclear F-actin scaffold stabilizes ribonucleoprotein
1357 droplets against gravity in large cells, *Nat. Cell Biol.*, 15 (2013) 1253-1259.

1358 [38] S. Elbaum-Garfinkle, Y. Kim, K. Szczepaniak, C.C.-H. Chen, C.R. Eckmann, S. Myong,
1359 C.P. Brangwynne, The disordered P granule protein LAF-1 drives phase separation into
1360 droplets with tunable viscosity and dynamics, *Proc. Natl. Acad. Sci. U. S. A.*, 112 (2015)
1361 7189-7194.

1362 [39] K.Y. Han, L. Graf, C.P. Reyes, B. Melkonian, R.A. Andersen, H.S. Yoon, M. Melkonian,
1363 A Re-investigation of *Sarcinochrysis marina* (Sarcinochrysidales, Pelagophyceae) from its
1364 Type Locality and the Descriptions of *Arachnochrysis*, *Pelagospilus*, *Sargassococcus* and
1365 *Sungminbooa* genera nov, *Protist*, 169 (2018) 79-106.

1366 [40] M.-T. Wei, S. Elbaum-Garfinkle, A.S. Holehouse, C.C.-H. Chen, M. Feric, C.B. Arnold,
1367 R.D. Priestley, R.V. Pappu, C.P. Brangwynne, Phase behaviour of disordered proteins
1368 underlying low density and high permeability of liquid organelles, *Nat. Chem.*, 9 (2017) 1118-
1369 1125.

1370 [41] T.S. Harmon, A.S. Holehouse, M.K. Rosen, R.V. Pappu, Intrinsically disordered linkers
1371 determine the interplay between phase separation and gelation in multivalent proteins, *Elife*,
1372 6 (2017) e30294.

1373 [42] A.K. Itakura, K.X. Chan, N. Atkinson, L. Pallesen, L. Wang, G. Reeves, W. Patena, O.
1374 Caspari, R. Roth, U. Goodenough, A.J. McCormick, H. Griffiths, M.C. Jonikas, A Rubisco-
1375 binding protein is required for normal pyrenoid number and starch sheath morphology in
1376 *Chlamydomonas reinhardtii*, *Proc. Natl. Acad. Sci. U. S. A.*, 116 (2019) 18445-18454.

1377 [43] L.M. Oltrogge, T. Chaijarasphong, A.W. Chen, E.R. Bolin, S. Marqusee, D.F. Savage,
1378 Multivalent interactions between CsoS2 and Rubisco mediate α -carboxysome formation,
1379 *Nat. Struct. Mol. Biol.*, 27 (2020) 281-287.

1380 [44] T. Wunder, S.L.H. Cheng, S.-K. Lai, H.-Y. Li, O. Mueller-Cajar, The phase separation
1381 underlying the pyrenoid-based microalgal Rubisco supercharger, *Nat. Commun.*, 9 (2018)
1382 5076.

1383 [45] M. Ludwig, D. Sültemeyer, G.D. Price, Isolation of *ccmKLMN* genes from the marine
1384 cyanobacterium, *Synechococcus* sp. PCC7002 (Cyanophyceae), and evidence that CcmM is
1385 essential for carboxysome assembly, *J. Phycol.*, 36 (2000) 1109-1119.

1386 [46] F. Cai, Z. Dou, S.L. Bernstein, R. Leverenz, E.B. Williams, S. Heinhorst, J. Shively, G.C.
1387 Cannon, C.A. Kerfeld, Advances in Understanding Carboxysome Assembly in
1388 *Prochlorococcus* and *Synechococcus* Implicate CsoS2 as a Critical Component, *Life*, 5
1389 (2015) 1141-1171.

1390 [47] H. Wang, X. Yan, H. Aigner, A. Bracher, N.D. Nguyen, W.Y. Hee, B.M. Long, G.D. Price,
1391 F.U. Hartl, M. Hayer-Hartl, Rubisco condensate formation by CcmM in β -carboxysome
1392 biogenesis, *Nature*, 566 (2019) 131-135.

- 1393 [48] A.H. Chen, A. Robinson-Mosher, D.F. Savage, P.A. Silver, J.K. Polka, The bacterial
1394 carbon-fixing organelle is formed by shell envelopment of preassembled cargo, PLoS One, 8
1395 (2013) e76127.
- 1396 [49] C.A. Kerfeld, M.R. Melnicki, Assembly, function and evolution of cyanobacterial
1397 carboxysomes, Current Opinion in Plant Biology, 31 (2016) 66-75.
- 1398 [50] J.C. Villarreal, S.S. Renner, Hornwort pyrenoids, carbon-concentrating structures,
1399 evolved and were lost at least five times during the last 100 million years, Proc. Natl. Acad.
1400 Sci. U. S. A., 109 (2012) 18873-18878.
- 1401 [51] L.C.M. Mackinder, M.T. Meyer, T. Mettler-Altmann, V.K. Chen, M.C. Mitchell, O.
1402 Caspari, E.S. Freeman Rosenzweig, L. Pallesen, G. Reeves, A. Itakura, R. Roth, F.
1403 Sommer, S. Geimer, T. Mühlhaus, M. Schroda, U. Goodenough, M. Stitt, H. Griffiths, M.C.
1404 Jonikas, A repeat protein links Rubisco to form the eukaryotic carbon-concentrating
1405 organelle, Proc. Natl. Acad. Sci. U. S. A., 113 (2016) 5958-5963.
- 1406 [52] M.D. Guiry, How Many Species of Algae Are There?, J. Phycol., 48 (2012) 1057-1063.
- 1407 [53] F. Burki, A.J. Roger, M.W. Brown, A.G.B. Simpson, The New Tree of Eukaryotes,
1408 Trends Ecol. Evol., 35 (2020) 43-55.
- 1409 [54] M. Sato, Y. Mogi, T. Nishikawa, S. Miyamura, T. Nagumo, S. Kawano, The dynamic
1410 surface of dividing cyanelles and ultrastructure of the region directly below the surface in
1411 *Cyanophora paradoxa*, Planta, 229 (2009) 781.
- 1412 [55] R.M. McKay, S.P. Gibbs, Phycoerythrin is absent from the pyrenoid of *Porphyridium*
1413 *cruentum*: photosynthetic implications, Planta, 180 (1990) 249-256.
- 1414 [56] I. Ohad, P. Siekevitz, G.E. Palade, Biogenesis of chloroplast membranes. I. Plastid
1415 dedifferentiation in a dark-grown algal mutant (*Chlamydomonas reinhardi*), J. Cell Biol., 35
1416 (1967) 521-552.
- 1417 [57] F.W. Li, J.C. Villarreal, P. Szovenyi, Hornworts: An Overlooked Window into Carbon-
1418 Concentrating Mechanisms, Trends Plant Sci., 22 (2017) 275-277.
- 1419 [58] P.L. Walne, H.J. Arnott, The comparative ultrastructure and possible function of
1420 eyespots: *Euglena granulata* and *Chlamydomonas eugametos*, Planta, 77 (1967) 325-353.
- 1421 [59] M. Tachibana, A.E. Allen, S. Kikutani, Y. Endo, C. Bowler, Y. Matsuda, Localization of
1422 putative carbonic anhydrases in two marine diatoms, *Phaeodactylum tricorutum* and
1423 *Thalassiosira pseudonana*, Photosynth. Res., 109 (2011) 205-221.
- 1424 [60] C. Zinssmeister, H. Keupp, G. Tischendorf, F. Kaulbars, M. Gottschling, Ultrastructure of
1425 calcareous dinophytes (Thoracosphaeraceae, Peridinales) with a focus on vacuolar crystal-
1426 like particles, PLoS One, 8 (2013) e54038.
- 1427 [61] S. Ota, K. Ueda, K.-I. Ishida, *Lotharella vacuolata* sp. nov., a new species of
1428 chlorarachniophyte algae, and time-lapse video observations on its unique post-cell division
1429 behavior, Phycological Res., 53 (2005) 275-286.
- 1430 [62] S.W. Nam, D. Go, M. Son, W. Shin, Ultrastructure of the flagellar apparatus in
1431 *Rhinomonas reticulata* var. *atorosea* (Cryptophyceae, Cryptophyta), Algae, 28 (2013) 331-
1432 341.
- 1433 [63] A.W.F. Schimper, Untersuchungen über die Chlorophyllkörper und die ihnen homologen
1434 Gebilde, Jahrb. wiss. Bot, 16 (1885) 1-247.
- 1435 [64] R. Wagner, Einige bemerkungen und fragen über das keimbläschen (vesicular
1436 germinativa), Müller's Archiv Anat Physiol Wissenschaft Med, 268 (1835) 373-377.
- 1437 [65] F. Schmitz, Die chromatophoren der algen: Vergleichende untersuchungen über bau
1438 und entwicklung der chlorophyllkörper und der analogen farbstoffkörper der algen, M. Cohen
1439 & Sohn (F. Cohen), Place Published, 1882.
- 1440 [66] R.H. Holdsworth, The isolation and partial characterization of the pyrenoid protein of
1441 *Eremosphaera viridis*, J. Cell Biol., 51 (1971) 499-513.
- 1442 [67] U.W. Goodenough, R. Levine, Chloroplast structure and function in ac-20, a mutant
1443 strain of *Chlamydomonas reinhardi*. 3. Chloroplast ribosomes and membrane organization,
1444 J. Cell Biol., 44 (1970) 547-562.
- 1445 [68] N.W. Kerby, L.V. Evans, Isolation and partial characterization of pyrenoids from the
1446 brown alga *Pilayella littoralis* (L.) Kjellm, Planta, 142 (1978) 91-95.

1447 [69] J.L. Salisbury, G.L. Floyd, Molecular, enzymatic and ultrastructure characterization of
1448 the scaly green monad *Micromonas squamata*, *Journal of Phycology*, 14 (1978) 362-368.

1449 [70] G. Lacoste-Royal, S.P. Gibbs, Immunocytochemical localization of ribulose-1, 5-
1450 biphosphate carboxylase in the pyrenoid and thylakoid region of the chloroplast of
1451 *Chlamydomonas reinhardtii*, *Plant Physiology*, 83 (1987) 602-606.

1452 [71] M.G. Vladimirova, A.G. Markelova, V.E. Semenenko, Use of the cytoimmunofluorescent
1453 method to clarify localization of ribulose biphosphate carboxylase in pyrenoids of unicellular
1454 algae, *Fiziol Rast*, 29 (1982) 725-734.

1455 [72] K. Kuchitsu, M. Tsuzuki, S. Miyachi, Polypeptide composition and enzyme activities of
1456 the pyrenoid and its regulation by CO₂ concentration in unicellular green algae, *Can. J. Bot.*,
1457 69 (1991) 1062-1069.

1458 [73] Z. Ramazanov, M. Rawat, M.C. Henk, C.B. Mason, S.W. Matthews, J.V. Moroney, The
1459 induction of the CO₂-concentrating mechanism is correlated with the formation of the starch
1460 sheath around the pyrenoid of *Chlamydomonas reinhardtii*, *Planta*, 195 (1994) 210–216.

1461 [74] K. Palmqvist, Photosynthetic CO₂-use efficiency in lichens and their isolated
1462 photobionts: the possible role of a CO₂-concentrating mechanism, *Planta*, 191 (1993) 48-56.

1463 [75] M.R. Badger, H. Pfanz, B. Büdel, U. Heber, O.L. Lange, Evidence for the functioning of
1464 photosynthetic CO₂-concentrating mechanisms in lichens containing green algal and
1465 cyanobacterial photobionts, *Planta*, 191 (1993) 57-70.

1466 [76] P.-A. Dangeard, Recherches sur les algues inférieures, *Ann Sci Nat Bot Ser VII*, 7
1467 (1888) 105-175.

1468 [77] M.T. Meyer, C. Whittaker, H. Griffiths, The algal pyrenoid: key unanswered questions, *J.*
1469 *Exp. Bot.*, 68 (2017) 3739-3749.

1470 [78] P.A. Salomé, S.S. Merchant, A Series of Fortunate Events: Introducing *Chlamydomonas*
1471 as a Reference Organism, *Plant Cell*, 31 (2019) 1682–1707.

1472 [79] B.D. Engel, M. Schaffer, L. Kuhn Cuellar, E. Villa, J.M. Pnitzko, W. Baumeister, Native
1473 architecture of the *Chlamydomonas* chloroplast revealed by in situ cryo-electron tomography,
1474 *Elife*, 4 (2015) e04889.

1475 [80] L.C.M. Mackinder, C. Chen, R.D. Leib, W. Patena, S.R. Blum, M. Rodman, S. Ramundo,
1476 C.M. Adams, M.C. Jonikas, A Spatial Interactome Reveals the Protein Organization of the
1477 Algal CO₂-Concentrating Mechanism, *Cell*, 171 (2017) 133-147.e114.

1478 [81] Y. Zhan, C.H. Marchand, A. Maes, A. Mauries, Y. Sun, J.S. Dhaliwal, J. Uniacke, S.
1479 Arragain, H. Jiang, N.D. Gold, V.J.J. Martin, S.D. Lemaire, W. Zerges, Pyrenoid functions
1480 revealed by proteomics in *Chlamydomonas reinhardtii*, *PLoS One*, 13 (2018) e0185039.

1481 [82] A. Küken, F. Sommer, L. Yaneva-Roder, L.C. Mackinder, M. Höhne, S. Geimer, M.C.
1482 Jonikas, M. Schroda, M. Stitt, Z. Nikoloski, T. Mettler-Altmann, Effects of
1483 microcompartmentation on flux distribution and metabolic pools in *Chlamydomonas*
1484 *reinhardtii* chloroplasts, *Elife*, 7 (2018) e37960.

1485 [83] W. Wietrzynski, M. Schaffer, D. Tegunov, S. Albert, A. Kanazawa, J.M. Pnitzko, W.
1486 Baumeister, B.D. Engel, Charting the native architecture of *Chlamydomonas* thylakoid
1487 membranes with single-molecule precision, *Elife*, 9 (2020) e53740.

1488 [84] A. Mukherjee, C.S. Lau, C.E. Walker, A.K. Rai, C.I. Prejean, G. Yates, T. Emrich-Mills,
1489 S.G. Lemoine, D.J. Vinyard, L.C.M. Mackinder, J.V. Moroney, Thylakoid localized
1490 bestrophin-like proteins are essential for the CO₂ concentrating mechanism of
1491 *Chlamydomonas reinhardtii*, *Proc. Natl. Acad. Sci. U. S. A.*, 116 (2019) 16915-16920.

1492 [85] M. Mitra, S.M. Lato, R.A. Ynalvez, Y. Xiao, J.V. Moroney, Identification of a new
1493 chloroplast carbonic anhydrase in *Chlamydomonas reinhardtii*, *Plant Physiol.*, 135 (2004)
1494 173-182.

1495 [86] D. Duanmu, Y. Wang, M.H. Spalding, Thylakoid lumen carbonic anhydrase (CAH3)
1496 mutation suppresses air-Dier phenotype of LCIB mutant in *Chlamydomonas reinhardtii*, *Plant*
1497 *Physiol.*, 149 (2009) 929-937.

1498 [87] M.A. Sinetova, E.V. Kupriyanova, A.G. Markelova, S.I. Allakhverdiev, N.A. Pronina,
1499 Identification and functional role of the carbonic anhydrase Cah3 in thylakoid membranes of
1500 pyrenoid of *Chlamydomonas reinhardtii*, *Biochim. Biophys. Acta*, 1817 (2012) 1248-1255.

1501 [88] R.M.L. McKay, S.P. Gibbs, Composition and function of pyrenoids: cytochemical and
1502 immunocytochemical approaches, *Can. J. Bot.*, 69 (1991) 1040-1052.

1503 [89] K. Kuchitsu, M. Tsuzuki, S. Miyachi, Changes of Starch Localization within the
1504 Chloroplast Induced by Changes in CO₂ Concentration during Growth of *Chlamydomonas*
1505 *reinhardtii*: Independent Regulation of Pyrenoid Starch and Stroma Starch, *Plant Cell*
1506 *Physiol.*, 29 (1988) 1269-1278.

1507 [90] A. Villarejo, F. Martinez, M. Pino Plumed, Z. Ramazanov, The induction of the CO₂
1508 concentrating mechanism in a starch-less mutant of *Chlamydomonas reinhardtii*, *Physiol.*
1509 *Plant.*, 98 (1996) 798-802.

1510 [91] C. Toyokawa, T. Yamano, H. Fukuzawa, Pyrenoid Starch Sheath Is Required for LCIB
1511 Localization and the CO₂-Concentrating Mechanism in Green Algae, *Plant Physiol.*, 182
1512 (2020) 1883-1893.

1513 [92] T. Yamano, T. Tsujikawa, K. Hatano, S.-I. Ozawa, Y. Takahashi, H. Fukuzawa, Light
1514 and Low-CO₂-Dependent LCIB–LCIC Complex Localization in the Chloroplast Supports the
1515 Carbon-Concentrating Mechanism in *Chlamydomonas reinhardtii*, *Plant Cell Physiol.*, 51
1516 (2010) 1453-1468.

1517 [93] Y. Wang, D.J. Stessman, M.H. Spalding, The CO₂ concentrating mechanism and
1518 photosynthetic carbon assimilation in limiting CO₂: how *Chlamydomonas* works against the
1519 gradient, *Plant J.*, 82 (2015) 429–448.

1520 [94] S. Jin, J. Sun, T. Wunder, D. Tang, A.B. Cousins, S.K. Sze, O. Mueller-Cajar, Y.-G.
1521 Gao, Structural insights into the LCIB protein family reveals a new group of β -carbonic
1522 anhydrases, *Proc. Natl. Acad. Sci. U. S. A.*, 113 (2016) 14716-14721.

1523 [95] S. He, H.-T. Chou, D. Matthies, T. Wunder, M.T. Meyer, N. Atkinson, A. Martinez-
1524 Sanchez, P.D. Jeffrey, S.A. Port, W. Patena, G. He, V.K. Chen, F.M. Hughson, A.J.
1525 McCormick, O. Mueller-Cajar, B.D. Engel, Z. Yu, M.C. Jonikas, The Structural Basis of
1526 Rubisco Phase Separation in the Pyrenoid, *Nature Plants*, 6 (2020) 1480-1490.

1527 [96] T.K. Antal, I.B. Kovalenko, A.B. Rubin, E. Tyystjärvi, Photosynthesis-related quantities
1528 for education and modeling, *Photosynth. Res.*, 117 (2013) 1-30.

1529 [97] N. Atkinson, C.N. Velanis, T. Wunder, D.J. Clarke, O. Mueller-Cajar, A.J. McCormick,
1530 The pyrenoidal linker protein EPYC1 phase separates with hybrid Arabidopsis-
1531 *Chlamydomonas* Rubisco through interactions with the algal Rubisco small subunit, *J. Exp.*
1532 *Bot.*, 70 (2019) 5271-5285.

1533 [98] M.T. Meyer, T. Genkov, J.N. Skepper, J. Jouhet, M.C. Mitchell, R.J. Spreitzer, H.
1534 Griffiths, Rubisco small-subunit α -helices control pyrenoid formation in *Chlamydomonas*,
1535 *Proc. Natl. Acad. Sci. U. S. A.*, 109 (2012) 19474-19479.

1536 [99] J.S. MacCready, J.L. Basalla, A.G. Vecchiarelli, Origin and Evolution of Carboxysome
1537 Positioning Systems in Cyanobacteria, *Mol. Biol. Evol.*, 37 (2020) 1434-1451.

1538 [100] M.M.M. Goudet, D.J. Orr, M. Melkonian, K.H. Müller, M.T. Meyer, E. Carmo-Silva, H.
1539 Griffiths, Rubisco and carbon concentrating mechanism (CCM) co-evolution across
1540 Chlorophyte and Streptophyte green algae, *New Phytol.*, 227 (2020) 810-823.

1541 [101] M.T. Meyer, A.K. Itakura, W. Patena, L. Wang, S. He, T. Emrich-Mills, C.S. Lau, G.
1542 Yates, L.C.M. Mackinder, M.C. Jonikas, Assembly of the algal CO₂-fixing organelle, the
1543 pyrenoid, is guided by a Rubisco-binding motif, *Science Advances*, 6 (2020) eabd2408.

1544 [102] E. Voronina, G. Seydoux, P. Sassone-Corsi, I. Nagamori, RNA granules in germ cells,
1545 *Cold Spring Harb. Perspect. Biol.*, 3 (2011) a002774.

1546 [103] M. Wilsch-Bräuninger, H. Schwarz, C. Nüsslein-Volhard, A sponge-like structure
1547 involved in the association and transport of maternal products during *Drosophila oogenesis*,
1548 *J. Cell Biol.*, 139 (1997) 817-829.

1549 [104] M.J. Snee, P.M. Macdonald, Dynamic organization and plasticity of sponge bodies,
1550 *Dev. Dyn.*, 238 (2009) 918-930.

1551 [105] X. Su, J.A. Ditlev, E. Hui, W. Xing, S. Banjade, J. Okrut, D.S. King, J. Taunton, M.K.
1552 Rosen, R.D. Vale, Phase separation of signaling molecules promotes T cell receptor signal
1553 transduction, *Science*, 352 (2016) 595-599.

1554 [106] S. Banjade, M.K. Rosen, Phase transitions of multivalent proteins can promote
1555 clustering of membrane receptors, *Elife*, 3 (2014) e04123.

1556 [107] H.B. Schmidt, D. Görlich, Transport Selectivity of Nuclear Pores, Phase Separation,
1557 and Membraneless Organelles, *Trends Biochem. Sci.*, 41 (2016) 46-61.

1558 [108] J.E. Lee, P.I. Cathey, H. Wu, R. Parker, G.K. Voeltz, Endoplasmic reticulum contact
1559 sites regulate the dynamics of membraneless organelles, *Science*, 367 (2020) eaay7108.

1560 [109] W. Ma, C. Mayr, A Membraneless Organelle Associated with the Endoplasmic
1561 Reticulum Enables 3'UTR-Mediated Protein-Protein Interactions, *Cell*, 175 (2018) 1492-
1562 1506.e1419.

1563 [110] Y. Fujioka, J. Alam, D. Noshiro, K. Mouri, T. Ando, Y. Okada, A.I. May, R.L. Knorr, K.
1564 Suzuki, Y. Ohsumi, N.N. Noda, Phase separation organizes the site of autophagosome
1565 formation, *Nature*, 578 (2020) 301-305.

1566 [111] D. Milovanovic, Y. Wu, X. Bian, P. De Camilli, A liquid phase of synapsin and lipid
1567 vesicles, *Science*, 361 (2018) 604-607.

1568 [112] W.F. Zeno, U. Baul, W.T. Snead, A.C.M. DeGroot, L. Wang, E.M. Lafer, D. Thirumalai,
1569 J.C. Stachowiak, Synergy between intrinsically disordered domains and structured proteins
1570 amplifies membrane curvature sensing, *Nat. Commun.*, 9 (2018) 4152.

1571 [113] W.F. Zeno, A.S. Thatte, L. Wang, W.T. Snead, E.M. Lafer, J.C. Stachowiak, Molecular
1572 Mechanisms of Membrane Curvature Sensing by a Disordered Protein, *J. Am. Chem. Soc.*,
1573 141 (2019) 10361-10371.

1574 [114] L. Boudière, M. Michaud, D. Petroustos, F. Rébeillé, D. Falconet, O. Bastien, S. Roy,
1575 G. Finazzi, N. Rolland, J. Jouhet, M.A. Block, E. Maréchal, Glycerolipids in photosynthesis:
1576 Composition, synthesis and trafficking, *Biochimica et Biophysica Acta (BBA) - Bioenergetics*,
1577 1837 (2014) 470-480.

1578 [115] H. Kirchhoff, U. Mukherjee, H.J. Galla, Molecular architecture of the thylakoid
1579 membrane: lipid diffusion space for plastoquinone, *Biochemistry*, 41 (2002) 4872-4882.

1580 [116] B. Andersson, J.M. Anderson, Lateral heterogeneity in the distribution of chlorophyll-
1581 protein complexes of the thylakoid membranes of spinach chloroplasts, *Biochim. Biophys.*
1582 *Acta*, 593 (1980) 427-440.

1583 [117] A.M. Pyszniak, S.P. Gibbs, Immunocytochemical localization of photosystem I and the
1584 fucoxanthin-chlorophylla/c light-harvesting complex in the diatom *Phaeodactylum*
1585 *tricornutum*, *Protoplasma*, 166 (1992) 208-217.

1586 [118] I. Tsekos, F.X. Niell, J. Aguilera, F. Lopez-Figueroa, S.G. Delivopoulos, Ultrastructure
1587 of the vegetative gametophytic cells of *Porphyra leucosticta* (Rhodophyta) grown in red, blue
1588 and green light, *Phycological Res.*, 50 (2002) 251-264.

1589 [119] F. Yuan, H. Alimohamadi, B. Bakka, A.N. Trementozzi, N.L. Fawzi, P. Rangamani, J.C.
1590 Stachowiak, Membrane bending by protein phase separation, *bioRxiv*, (2020)
1591 10.1101/2020.05.21.109751.

1592 [120] O.D. Caspari, M.T. Meyer, D. Tolleter, T.M. Wittkopp, N.J. Cunniffe, T. Lawson, A.R.
1593 Grossman, H. Griffiths, Pyrenoid loss in *Chlamydomonas reinhardtii* causes limitations in
1594 CO₂ supply, but not thylakoid operating efficiency, *J. Exp. Bot.*, 68 (2017) 3903-3913.

1595 [121] A. Mechela, S. Schwenkert, J. Soll, A brief history of thylakoid biogenesis, *Open Biol.*,
1596 9 (2019) 180237.

1597 [122] D.J. Griffiths, The pyrenoid, *Bot. Rev.*, 36 (1970) 29-58.

1598 [123] K. Chan, Ultrastructure of Pyrenoid Division in *Coelastrum* sp., *Cytologia*, 39 (1974)
1599 531-536.

1600 [124] L.R. Hoffman, Observations on the fine structure of Oedogonium. V. Evidence for the
1601 de novo Formation of Pyrenoids in Zoospores of *OE. cardiacum*, *J. Phycol.*, 4 (1968) 212-
1602 218.

1603 [125] B. Retallack, R.D. Butler, The development and structure of pyrenoids in *Bulbochaete*
1604 *hiloensis*, *J. Cell Sci.*, 6 (1970) 229-241.

1605 [126] T. Ohiwa, Observations on chloroplast growth and pyrenoid formation in *Spirogyra*. A
1606 study by means of uncoiled picture of chloroplast, *Bot Mag Tokyo*, 89 (1976) 259-266.

1607 [127] E. Gantt, S.F. Conti, The ultrastructure of *Porphyridium cruentum*, *J. Cell Biol.*, 26
1608 (1965) 365-381.

1609 [128] T. Hori, I. Inouye, The ultrastructure of mitosis in *Cricosphaera roscoffensis* var.
1610 *haptoneofera* (Prymnesiophyceae), *Protoplasma*, 106 (1981) 121-135.

1611 [129] K.L. Schornstein, J. Scott, Ultrastructure of cell division in the unicellular red alga
1612 *Porphyridium purpureum*, Can. J. Bot., 60 (1982) 85-97.

1613 [130] C.A. Lander, The Relation of the Plastid to Nuclear Division in *Anthoceros laevis*, Am.
1614 J. Bot., 22 (1935) 42-51.

1615 [131] L.V. Evans, Distribution of pyrenoids among some brown algae, J. Cell Sci., 1 (1966)
1616 449-454.

1617 [132] E.J. Cox, Observations on the morphology and vegetative cell division of the diatom
1618 *Donkinia recta*, Helgoländer Meeresuntersuchungen, 34 (1981) 497-506.

1619 [133] T. Osafune, A. Yokota, S. Sumida, E. Hase, Immunogold Localization of Ribulose-1,5-
1620 Bisphosphate Carboxylase with Reference to Pyrenoid Morphology in Chloroplasts of
1621 Synchronized *Euglena gracilis* Cells, Plant Physiol., 92 (1990) 802-808.

1622 [134] C. Nagasato, T. Motomura, New Pyrenoid Formation in the Brown Alga, *Scytosiphon*
1623 *lomentaria* (Scytosiphonales, Phaeophyceae), J. Phycol., 38 (2002) 800-806.

1624 [135] F. McAllister, The Pyrenoids of *Anthoceros* and *Notothylas* with Especial Reference to
1625 Their Presence in Spore Mother Cells, Am. J. Bot., 14 (1927) 246-257.

1626 [136] C.N. Sun, Submicroscopic structure and development of the chloroplast and pyrenoid
1627 in *Anthoceros laevis*, Protoplasma, 55 (1962) 89-98.

1628 [137] K. Ueda, The Pyrenoid of *Chlorogonium elongatum*, in: H. Tamiya (Ed.) Studies on
1629 Microalgae and Photosynthetic Bacteria: A Collection of Papers Dedicated to Hiroshi Tamiya
1630 on the Occasion of His 60th Birthday, Japanese Society of Plant Physiologists, University of
1631 Tokyo Press, Tokyo, 1963, pp. 636.

1632 [138] G.M. Smith, Cytological Studies in the Protococcales. III. Cell Structure and Autospore
1633 Formation in *Tetraedron minimum* (A. Br.), Hansg, Ann. Bot., 32 (1918) 459-464.

1634 [139] M. Vítová, J. Hendrychová, M. Čížková, V. Cepak, J.G. Umen, V. Zachleder, K. Bišová,
1635 Accumulation, activity and localization of cell cycle regulatory proteins and the chloroplast
1636 division protein FtsZ in the alga *Scenedesmus quadricauda* under inhibition of nuclear DNA
1637 replication, Plant Cell Physiol., 49 (2008) 1805-1817.

1638 [140] K.C. Vaughn, E.O. Campbell, J. Hasegawa, H.A. Owen, K.S. Renzaglia, The pyrenoid
1639 is the site of ribulose 1,5-bisphosphate carboxylase/oxygenase accumulation in the hornwort
1640 (Bryophyta: Anthocerotae) chloroplast, Protoplasma, 156 (1990) 117-129.

1641 [141] U.W. Goodenough, Chloroplast Division and Pyrenoid Formation in *Chlamydomonas*
1642 *reinhardi*, J. Phycol., 6 (1970) 1-6.

1643 [142] I. Manton, Further observations on the fine structure of *Chrysochromulina chiton* with
1644 special reference to the haptonema, 'peculiar' golgi structure and scale production, J. Cell
1645 Sci., 2 (1967) 265-272.

1646 [143] S. Schuette, K.S. Renzaglia, Development of multicellular spores in the hornwort genus
1647 *Dendroceros* (Dendrocerotaceae, Anthocerotophyta) and the occurrence of endospory in
1648 Bryophytes, Nova Hedwigia, 91 (2010) 301-316.

1649 [144] R. Subrahmanyam, On the cell-division and mitosis in some South Indian diatoms,
1650 Proc. Indian Acad. Sci., 22 (1945) 331-354.

1651 [145] D.G. Mann, In vivo Observations of Plastid and Cell Division in Raphid Diatoms and
1652 Their Relevance to Diatom Systematics, Ann. Bot., 55 (1985) 95-108.

1653 [146] A. Tanaka, C. Nagasato, S. Uwai, T. Motomura, H. Kawai, Re-examination of
1654 ultrastructures of the stellate chloroplast organization in brown algae: Structure and
1655 development of pyrenoids, Phycological Res., 55 (2007) 203-213.

1656 [147] L.M. Patrone, S.T. Broadwater, J.L. Scott, Ultrastructure of vegetative and dividing cells
1657 of the unicellular red algae *Rhodella violacea* and *Rhodella maculata*, J. Phycol., 27 (1991)
1658 742-753.

1659 [148] A. Jenks, S.P. Gibbs, Immunolocalization and distribution of form ii rubisco in the
1660 pyrenoid and chloroplast stroma of *Amphidinium carterae* and form i rubisco in the symbiont-
1661 derived plastids of *Peridinium foliaceum* (dinophyceae), J. Phycol., 36 (2000) 127-138.

1662 [149] U.G. Johnson, K.R. Porter, Fine Structure of Cell Division in *Chlamydomonas reinhardi*:
1663 Basal Bodies and Microtubules, Journal of Cell Biology, 38 (1968) 403-425.

1664 [150] E.T. O'Toole, S.K. Dutcher, Site-specific basal body duplication in *Chlamydomonas*,
1665 Cytoskeleton (Hoboken), 71 (2014) 108-118.

1666 [151] S. Vitha, R.S. McAndrew, K.W. Osteryoung, FtsZ ring formation at the chloroplast
1667 division site in plants, *J. Cell Biol.*, 153 (2001) 111-120.

1668 [152] A.D. TerBush, Y. Yoshida, K.W. Osteryoung, FtsZ in chloroplast division: structure,
1669 function and evolution, *Curr. Opin. Cell Biol.*, 25 (2013) 461-470.

1670 [153] K. Kanamaru, M. Fujiwara, M. Kim, A. Nagashima, E. Nakazato, K. Tanaka, H.
1671 Takahashi, Chloroplast targeting, distribution and transcriptional fluctuation of AtMinD1, a
1672 Eubacteria-type factor critical for chloroplast division, *Plant Cell Physiol.*, 41 (2000) 1119-
1673 1128.

1674 [154] F. van den Ent, L. Amos, J. Löwe, Bacterial ancestry of actin and tubulin, *Curr. Opin.*
1675 *Microbiol.*, 4 (2001) 634-638.

1676 [155] T. Wakasugi, T. Nagai, M. Kapoor, M. Sugita, M. Ito, S. Ito, J. Tsudzuki, K. Nakashima,
1677 T. Tsudzuki, Y. Suzuki, A. Hamada, T. Ohta, A. Inamura, K. Yoshinaga, M. Sugiura,
1678 Complete nucleotide sequence of the chloroplast genome from the green alga *Chlorella*
1679 *vulgaris*: the existence of genes possibly involved in chloroplast division, *Proc. Natl. Acad.*
1680 *Sci. U. S. A.*, 94 (1997) 5967-5972.

1681 [156] Y. Hu, Z.-W. Chen, W.-Z. Liu, X.-L. Liu, Y.-K. He, Chloroplast division is regulated by
1682 the circadian expression of FTSZ and MIN genes in *Chlamydomonas reinhardtii*, *Eur. J.*
1683 *Phycol.*, 43 (2008) 207-215.

1684 [157] Y. Hirakawa, K.-I. Ishida, Prospective function of FtsZ proteins in the secondary plastid
1685 of chlorarachniophyte algae, *BMC Plant Biol.*, 15 (2015) 276.

1686 [158] B.T. Hovde, C. Deodato, R.A. Andersen, S. Starkenburg, R.A. Cattolico, others,
1687 *Chrysochromulina*: Genomic assessment and taxonomic diagnosis of the type species for an
1688 oleaginous algal clade, *Algal Res*, 37 (2019) 307-319.

1689 [159] S.-Y. Miyagishima, K. Suzuki, K. Okazaki, Y. Kabeya, Expression of the nucleus-
1690 encoded chloroplast division genes and proteins regulated by the algal cell cycle, *Mol. Biol.*
1691 *Evol.*, 29 (2012) 2957-2970.

1692 [160] R. Onuma, N. Mishra, S.-Y. Miyagishima, Regulation of chloroplast and nucleomorph
1693 replication by the cell cycle in the cryptophyte *Guillardia theta*, *Sci. Rep.*, 7 (2017) 2345.

1694 [161] D.C. Price, U.W. Goodenough, R. Roth, J.-H. Lee, T. Kariyawasam, M. Mutwil, C.
1695 Ferrari, F. Facchinelli, S.G. Ball, U. Cenci, C.X. Chan, N.E. Wagner, H.S. Yoon, A.P.M.
1696 Weber, D. Bhattacharya, Analysis of an improved *Cyanophora paradoxa* genome assembly,
1697 *DNA Res.*, 26 (2019) 287-299.

1698 [162] N. Sumiya, A. Hirata, S. Kawano, Multiple FtsZ Ring Formation and Reduplicated
1699 Chloroplast DNA in *Nannochloris bacillaris* (Chlorophyta, Trebouxiophyceae) Under
1700 Phosphate-enriched Culture, *J. Phycol.*, 44 (2008) 1476-1489.

1701 [163] N. Sumiya, S. Owari, K. Watanabe, S. Kawano, Role of Multiple FtsZ Rings in
1702 Chloroplast Division Under Oligotrophic and Eutrophic Conditions in the Unicellular Green
1703 Algal *Nannochloris bacillaris* (Chlorophyta, Trebouxiophyceae), *J. Phycol.*, 48 (2012) 1187-
1704 1196.

1705 [164] M. Onishi, J.G. Umen, F.R. Cross, J.R. Pringle, Cleavage-furrow formation without F-
1706 actin in *Chlamydomonas*, *Proc. Natl. Acad. Sci. U. S. A.*, (2020).

1707 [165] T. Mita, T. Kuroiwa, Division of Plastids by a Plastid-Dividing Ring in *Cyanidium*
1708 *caldarium*, in: M. Tazawa (Ed.) *Cell Dynamics: Cytoplasmic Streaming Cell Movement—*
1709 *Contraction and Migration Cell and Organelle Division Phototaxis of Cell and Cell Organelle*,
1710 Springer Vienna, Place Published, 1989, pp. 133-152.

1711 [166] H. Hashimoto, Involvement of actin filaments in chloroplast division of the alga
1712 *Closterium ehrenbergii*, *Protoplasma*, 167 (1992) 88-96.

1713 [167] J.D. Harper, D.W. McCurdy, M.A. Sanders, J.L. Salisbury, P.C. John, Actin dynamics
1714 during the cell cycle in *Chlamydomonas reinhardtii*, *Cell Motil. Cytoskeleton*, 22 (1992) 117-
1715 126.

1716 [168] G.O. Wasteneys, D.A. Collings, B.E.S. Gunning, P.K. Hepler, D. Menzel, Actin in living
1717 and fixed characean internodal cells: identification of a cortical array of fine actin strands and
1718 chloroplast actin rings, *Protoplasma*, 190 (1996) 25-38.

1719 [169] D.E. Wujek, K.E. Camburn, H.T. Andrews, An ultrastructural study of pyrenoids in
1720 *Leptosiropsis torulosa*, *Protoplasma*, 86 (1975) 263-268.

1721 [170] G.M. Lokhorst, W. Star, Pyrenoid Ultrastructure in *Ulothrix* (Chlorophyceae), *Acta Bot.*
1722 *Neerl.*, 29 (1980) 1-15.

1723 [171] A. Giustiniani, W. Drenckhan, C. Poulard, Interfacial tension of reactive, liquid
1724 interfaces and its consequences, *Adv. Colloid Interface Sci.*, 247 (2017) 185-197.

1725 [172] R.M. Brown, H.C. Bold, R.N. Lester, Comparative studies of the algal genera
1726 *Tetracystis* and *Chlorococcum*, University of Texas, Place Published, 1964.

1727 [173] F. McAllister, The Pyrenoid of *Anthoceros*, *Am. J. Bot.*, 1 (1914) 79-95.

1728 [174] T. Bisalputra, T.E. Weier, The pyrenoid of *Scenedesmus quadricauda*, *Am. J. Bot.*, 51
1729 (1964) 881-892.

1730 [175] M. Hofweber, D. Dormann, Friend or foe—Post-translational modifications as
1731 regulators of phase separation and RNP granule dynamics, *J. Biol. Chem.*, 294 (2019) 7137-
1732 7150.

1733 [176] A. Bah, J.D. Forman-Kay, Modulation of Intrinsically Disordered Protein Function by
1734 Post-translational Modifications, *J. Biol. Chem.*, 291 (2016) 6696-6705.

1735 [177] A. Wang, A.E. Conicella, H.B. Schmidt, E.W. Martin, S.N. Rhoads, A.N. Reeb, A.
1736 Nourse, D. Ramirez Montero, V.H. Ryan, R. Rohatgi, Others, A single N-terminal
1737 phosphomimic disrupts TDP-43 polymerization, phase separation, and RNA splicing, *EMBO*
1738 *J.*, 37 (2018) e97452.

1739 [178] J. Söding, D. Zwicker, S. Sohrabi-Jahromi, M. Boehning, J. Kirschbaum, Mechanisms
1740 for Active Regulation of Biomolecular Condensates, *Trends in Cell Biology*, 30 (2020) 4-14.

1741 [179] D. Zwicker, R. Seyboldt, C.A. Weber, A.A. Hyman, F. Jülicher, Growth and division of
1742 active droplets provides a model for protocells, *Nat. Phys.*, 13 (2017) 408-413.

1743 [180] M.V. Turkina, A. Blanco-Rivero, J.P. Vainonen, A.V. Vener, A. Villarejo, CO₂ limitation
1744 induces specific redox-dependent protein phosphorylation in *Chlamydomonas reinhardtii*,
1745 *Proteomics*, 6 (2006) 2693-2704.

1746 [181] H. Wang, B. Gau, W.O. Slade, M. Juergens, P. Li, L.M. Hicks, The global
1747 phosphoproteome of *Chlamydomonas reinhardtii* reveals complex organellar
1748 phosphorylation in the flagella and thylakoid membrane, *Mol. Cell. Proteomics*, 13 (2014)
1749 2337-2353.

1750 [182] E.P. Bentley, B.B. Frey, A.A. Deniz, Physical Chemistry of Cellular Liquid-Phase
1751 Separation, *Chem. Eur. J.*, 25 (2019) 5600-5610.

1752 [183] T. Wunder, Z.G. Oh, O. Mueller-Cajar, CO₂-fixing liquid droplets: towards a dissection
1753 of the microalgal pyrenoid, *Traffic*, 20 (2019) 380-389.

1754 [184] K.L. Pennington, T.Y. Chan, M.P. Torres, J.L. Andersen, The dynamic and stress-
1755 adaptive signaling hub of 14-3-3: emerging mechanisms of regulation and context-dependent
1756 protein–protein interactions, *Oncogene*, 37 (2018) 5587-5604.

1757 [185] T. Obsil, V. Obsilova, Structural basis of 14-3-3 protein functions, *Semin. Cell Dev.*
1758 *Biol.*, 22 (2011) 663-672.

1759 [186] A. Aitken, 14-3-3 proteins: a historic overview, *Semin. Cancer Biol.*, 16 (2006) 162-172.

1760 [187] C.W. Pak, M. Kosno, A.S. Holehouse, S.B. Padrick, A. Mittal, R. Ali, A.A. Yunus, D.R.
1761 Liu, R.V. Pappu, M.K. Rosen, Sequence Determinants of Intracellular Phase Separation by
1762 Complex Coacervation of a Disordered Protein, *Mol. Cell*, 63 (2016) 72-85.

1763 [188] B. Van Treeck, D.S.W. Protter, T. Matheny, A. Khong, C.D. Link, R. Parker, RNA self-
1764 assembly contributes to stress granule formation and defining the stress granule
1765 transcriptome, *Proc. Natl. Acad. Sci. U. S. A.*, 115 (2018) 2734-2739.

1766 [189] Y. Ma, S.V. Pollock, Y. Xiao, K. Cunnusamy, J.V. Moroney, Identification of a novel
1767 gene, CIA6, required for normal pyrenoid formation in *Chlamydomonas reinhardtii*, *Plant*
1768 *Physiol.*, 156 (2011) 884-896.

1769 [190] A.J. Brueggeman, D.S. Gangadharaiah, M.F. Cserhati, D. Casero, D.P. Weeks, I.
1770 Ladunga, Activation of the carbon concentrating mechanism by CO₂ deprivation coincides
1771 with massive transcriptional restructuring in *Chlamydomonas reinhardtii*, *Plant Cell*, 24
1772 (2012) 1860-1875.

1773 [191] W. Fang, Y. Si, S. Douglass, D. Casero, S.S. Merchant, M. Pellegrini, I. Ladunga, P.
1774 Liu, M.H. Spalding, Transcriptome-wide changes in *Chlamydomonas reinhardtii* gene

1775 expression regulated by carbon dioxide and the CO₂-concentrating mechanism regulator
1776 CIA5/CCM1, *Plant Cell*, 24 (2012) 1876-1893.

1777 [192] P. Cloutier, M. Lavallée-Adam, D. Faubert, M. Blanchette, B. Coulombe, A newly
1778 uncovered group of distantly related lysine methyltransferases preferentially interact with
1779 molecular chaperones to regulate their activity, *PLoS Genet.*, 9 (2013) e1003210.

1780 [193] O.N. Borkhsenius, C.B. Mason, J.V. Moroney, The intracellular localization of
1781 ribulose-1,5-bisphosphate Carboxylase/Oxygenase in *Chlamydomonas reinhardtii*, *Plant*
1782 *Physiol.*, 116 (1998) 1585-1591.

1783 [194] M.C. Mitchell, M.T. Meyer, H. Griffiths, Dynamics of carbon-concentrating mechanism
1784 induction and protein relocalization during the dark-to-light transition in synchronized
1785 *Chlamydomonas reinhardtii*, *Plant Physiol.*, 166 (2014) 1073-1082.

1786 [195] M.C. Munder, D. Midtvedt, T. Franzmann, E. Nüske, O. Otto, M. Herbig, E. Ulbricht, P.
1787 Müller, A. Taubenberger, S. Maharana, L. Malinowska, D. Richter, J. Guck, V. Zaburdaev, S.
1788 Alberti, A pH-driven transition of the cytoplasm from a fluid- to a solid-like state promotes
1789 entry into dormancy, *Elife*, 5 (2016) e09347.

1790 [196] T.M. Franzmann, M. Jahnel, A. Pozniakovsky, J. Mahamid, A.S. Holehouse, E. Nüske,
1791 D. Richter, W. Baumeister, S.W. Grill, R.V. Pappu, A.A. Hyman, S. Alberti, Phase separation
1792 of a yeast prion protein promotes cellular fitness, *Science*, 359 (2018) eaao5654.

1793 [197] T.J. Nott, E. Petsalaki, P. Farber, D. Jervis, E. Fussner, A. Plochowitz, T.D. Craggs,
1794 D.P. Bazett-Jones, T. Pawson, J.D. Forman-Kay, A.J. Baldwin, Phase transition of a
1795 disordered nuage protein generates environmentally responsive membraneless organelles,
1796 *Mol. Cell*, 57 (2015) 936-947.

1797 [198] J.A. Riback, C.D. Katanski, J.L. Kear-Scott, E.V. Pilipenko, A.E. Rojek, T.R. Sosnick,
1798 D.A. Drummond, Stress-Triggered Phase Separation Is an Adaptive, Evolutionarily Tuned
1799 Response, *Cell*, 168 (2017) 1028-1040.e1019.

1800 [199] K. Oglęcka, P. Rangamani, B. Liedberg, R.S. Kraut, A.N. Parikh, Oscillatory phase
1801 separation in giant lipid vesicles induced by transmembrane osmotic differentials, *Elife*, 3
1802 (2014) e03695.

1803 [200] J.V. Moroney, R.A. Ynalvez, Proposed carbon dioxide concentrating mechanism in
1804 *Chlamydomonas reinhardtii*, *Eukaryot. Cell*, 6 (2007) 1251-1259.

1805 [201] J.H. Hennacy, M.C. Jonikas, Prospects for Engineering Biophysical CO₂ Concentrating
1806 Mechanisms into Land Plants to Enhance Yields, *Annu. Rev. Plant Biol.*, 71 (2020) 461-485.

1807 [202] S. Kroschwald, M.C. Munder, S. Maharana, T.M. Franzmann, D. Richter, M. Ruer, A.A.
1808 Hyman, S. Alberti, Different Material States of Pub1 Condensates Define Distinct Modes of
1809 Stress Adaptation and Recovery, *Cell Rep.*, 23 (2018) 3327-3339.

1810 [203] T.K. Harris, G.J. Turner, Structural basis of perturbed pKa values of catalytic groups in
1811 enzyme active sites, *IUBMB Life*, 53 (2002) 85-98.

1812 [204] M. Vítová, K. Bišová, M. Hlavová, S. Kawano, V. Zachleder, M. Cížková,
1813 *Chlamydomonas reinhardtii*: duration of its cell cycle and phases at growth rates affected by
1814 temperature, *Planta*, 234 (2011) 599-608.

1815 [205] R.M. Morgan-Kiss, A.G. Ivanov, S. Modla, K. Czymmek, N.P.A. Hüner, J.C. Prisco, J.T.
1816 Lisle, T.E. Hanson, Identity and physiology of a new psychrophilic eukaryotic green alga,
1817 *Chlorella* sp., strain BI, isolated from a transitory pond near Bratina Island, Antarctica,
1818 *Extremophiles*, 12 (2008) 701-711.

1819 [206] B. Eddie, C. Krembs, S. Neuer, Characterization and growth response to temperature
1820 and salinity of psychrophilic, halotolerant *Chlamydomonas* sp. ARC isolated from Chukchi
1821 Sea ice, *Mar. Ecol. Prog. Ser.*, 354 (2008) 107-117.

1822 [207] S. Yau, A. Lopes Dos Santos, W. Eikrem, C. Gérikas Ribeiro, P. Gourvil, S. Balzano,
1823 M.-L. Escande, H. Moreau, D. Vaultot, *Mantoniella beaufortii* and *Mantoniella baffinensis* sp.
1824 nov. (Mamiellales, Mamiellophyceae), two new green algal species from the high arctic, *J.*
1825 *Phycol.*, 56 (2020) 37-51.

1826 [208] A. Kremp, M. Elbrächter, M. Schweikert, J.L. Wolny, M. Gottschling, *Woloszynskia*
1827 *halophila* (Biecheler) comb. nov.: A Bloom-forming Cold-water Dinoflagellate Co-occurring
1828 with *Scrippsiella hangoei* (Dinophyceae) in the Baltic Sea, *J. Phycol.*, 41 (2005) 629-642.

1829 [209] T. Horiguchi, M. Hoppenrath, *Haramonas viridis* sp. nov. (Raphidophyceae,
1830 Heterokontophyta), a new sand-dwelling raphidophyte from cold temperate waters,
1831 Phycological Res., 51 (2003) 61-67.

1832 [210] M. Cvetkovska, N.P.A. Hüner, D.R. Smith, Chilling out: the evolution and diversification
1833 of psychrophilic algae with a focus on *Chlamydomonadales*, Polar Biol., 40 (2017) 1169-
1834 1184.

1835 [211] B. Szyszka-Mroz, M. Cvetkovska, A.G. Ivanov, D.R. Smith, M. Possmayer, D.P.
1836 Maxwell, N.P.A. Hüner, Cold-Adapted Protein Kinases and Thylakoid Remodeling Impact
1837 Energy Distribution in an Antarctic Psychrophile, Plant Physiol., 180 (2019) 1291-1309.

1838 [212] L. Valledor, T. Furuhashi, A.-M. Hanak, W. Weckwerth, Systemic cold stress
1839 adaptation of *Chlamydomonas reinhardtii*, Mol. Cell. Proteomics, 12 (2013) 2032-2047.

1840 [213] A. Patel, L. Malinowska, S. Saha, J. Wang, S. Alberti, Y. Krishnan, A.A. Hyman, ATP as
1841 a biological hydrotrope, Science, 356 (2017) 753-756.

1842 [214] S.V. Pollock, S.L. Colombo, D.L. Prout, A.C. Godfrey, J.V. Moroney, Rubisco Activase
1843 Is Required for Optimal Photosynthesis in the Green Alga *Chlamydomonas reinhardtii* in a
1844 Low-CO₂ Atmosphere, Plant Physiol., 133 (2003) 1854-1861.

1845 [215] O. Mueller-Cajar, The Diverse AAA+ Machines that Repair Inhibited Rubisco Active
1846 Sites, Front Mol Biosci, 4 (2017) 31.

1847 [216] W. Yamori, C. Masumoto, H. Fukayama, A. Makino, Rubisco activase is a key
1848 regulator of non-steady-state photosynthesis at any leaf temperature and, to a lesser extent,
1849 of steady-state photosynthesis at high temperature, The Plant Journal, 71 (2012) 871-880.

1850 [217] R.M.L. McKay, S.P. Gibbs, K.C. Vaughn, RuBisCo activase is present in the pyrenoid
1851 of green algae, Protoplasma, 162 (1991) 38-45.

1852 [218] L. Wang, T. Yamano, S. Takane, Y. Niikawa, C. Toyokawa, S.-I. Ozawa, R. Tokutsu, Y.
1853 Takahashi, J. Minagawa, Y. Kanesaki, H. Yoshikawa, H. Fukuzawa, Chloroplast-mediated
1854 regulation of CO₂-concentrating mechanism by Ca²⁺-binding protein CAS in the green alga
1855 *Chlamydomonas reinhardtii*, Proc. Natl. Acad. Sci. U. S. A., 113 (2016) 12586-12591.

1856 [219] T. Yamano, C. Toyokawa, H. Fukuzawa, High-resolution suborganellar localization of
1857 Ca²⁺-binding protein CAS, a novel regulator of CO₂-concentrating mechanism, Protoplasma,
1858 255 (2018) 1015-1022.

1859 [220] B. Liu, B. Poolman, A.J. Boersma, Ionic Strength Sensing in Living Cells, ACS Chem.
1860 Biol., 12 (2017) 2510-2514.

1861 [221] L. Wang, T. Yamano, M. Kajikawa, M. Hirono, H. Fukuzawa, Isolation and
1862 characterization of novel high-CO₂-requiring mutants of *Chlamydomonas reinhardtii*,
1863 Photosynth. Res., 121 (2014) 175-184.

1864 [222] L. Teng, L. Ding, Q. Lu, Microscopic observation of pyrenoids in order Ulvales
1865 (Chlorophyta) collected from Qingdao coast, J. Ocean Univ. China, 10 (2011) 223-228.

1866 [223] I. Dehning, M.M. Tilzer, Survival of *Scenedesmus acuminatus* (Chlorophyceae) in
1867 Darkness, J. Phycol., 25 (1989) 509-515.

1868 [224] P.W. Voorhees, The theory of Ostwald ripening, J. Stat. Phys., 38 (1985) 231-252.

1869 [225] Y. Shin, Y.-C. Chang, D.S.W. Lee, J. Berry, D.W. Sanders, P. Ronceray, N.S.
1870 Wingreen, M. Haataja, C.P. Brangwynne, Liquid Nuclear Condensates Mechanically Sense
1871 and Restructure the Genome, Cell, 175 (2018) 1481-1491.e1413.

1872 [226] M.C. Mitchell, G. Metodieva, M.V. Metodiev, H. Griffiths, M.T. Meyer, Pyrenoid loss
1873 impairs carbon-concentrating mechanism induction and alters primary metabolism in
1874 *Chlamydomonas reinhardtii*, J. Exp. Bot., 68 (2017) 3891-3902.

1875 [227] R.J. Blank, R.K. Trench, Immunogold localization of Ribulose-1.5-bisphosphate
1876 carboxylase-oxygenase in *Symbiodinium kawahutii* trench et blank - An Endosymbiotic
1877 Dinoflagellate, Endocytobiosis Cell Res., 5 (1988) 75-82.

1878 [228] H. Kajikawa, M. Okada, F. Ishikawa, Y. Okada, K. Nakayama, Immunochemical
1879 Studies on Ribulose 1,5-Bisphosphate Carboxylase/Oxygenase in the Chloroplasts of the
1880 Marine Alga *Bryopsis maxima*, Plant Cell Physiol., 29 (1988) 549-556.

1881 [229] J.Z. Kiss, A.C. Vasoconcelos, R.E. Triemer, Paramylon Synthesis and Chloroplast
1882 Structure Associated with Nutrient Levels in *Euglena* (Euglenophyceae), J. Phycol., 22
1883 (1986) 327-333.

- 1884 [230] R.M.L. McKay, S.P. Gibbs, Immunocytochemical localization of ribulose 1,5-
1885 bisphosphate carboxylase/oxygenase in light-limited and light-saturated cells of *Chlorella*
1886 *pyrenoidosa*, Protoplasma, 149 (1989) 31-37.
- 1887 [231] L. Mustardy, F.X. Cunningham, E. Gantt, Localization and quantitation of chloroplast
1888 enzymes and light-harvesting components using immunocytochemical methods, Plant
1889 Physiol., 94 (1990) 334-340.
- 1890 [232] T. Osafune, S. Sumida, T. Ehara, E. Hase, Three-Dimensional Distribution of Ribulose-
1891 1,5-Bisphosphate Carboxylase/Oxygenase in Chloroplasts of Actively Photosynthesizing Cell
1892 of *Euglena gracilis*, J. Electron Microsc., 38 (1989) 399-402.
- 1893 [233] N. Nassoury, L. Fritz, D. Morse, Circadian changes in ribulose-1,5-bisphosphate
1894 carboxylase/oxygenase distribution inside individual chloroplasts can account for the rhythm
1895 in dinoflagellate carbon fixation, Plant Cell, 13 (2001) 923-934.
- 1896 [234] S. Lin, E.J. Carpenter, Rubisco of *Dunaliella tertiolecta* is redistributed between the
1897 pyrenoid and the stroma as a light /shade response, Mar. Biol., 127 (1997) 521-529.
- 1898 [235] J.A. Raven, M. Giordano, J. Beardall, S.C. Maberly, Algal evolution in relation to
1899 atmospheric CO₂: carboxylases, carbon-concentrating mechanisms and carbon oxidation
1900 cycles, Philos. Trans. R. Soc. Lond. B Biol. Sci., 367 (2012) 493-507.
- 1901 [236] E. Morita, M. Abe T Fau - Tsuzuki, S. Tsuzuki M Fau - Fujiwara, N. Fujiwara S Fau -
1902 Sato, A. Sato N Fau - Hirata, K. Hirata A Fau - Sonoike, H. Sonoike K Fau - Nozaki, H.
1903 Nozaki, Presence of the CO₂-concentrating mechanism in some species of the pyrenoid-less
1904 free-living algal genus *Chloromonas* (Volvocales, Chlorophyta), Planta, 204 (1998) 269-276.
- 1905 [237] J.C. Villarreal, K.S. Renzaglia, The hornworts: important advancements in early land
1906 plant evolution, J. Bryol., 37 (2015) 157-170.
- 1907 [238] A. Flamholz, P.M. Shih, Cell biology of photosynthesis over geologic time, Curr. Biol.,
1908 30 (2020) R490-R494.
- 1909 [239] J. Zhang, X.-X. Fu, R.-Q. Li, X. Zhao, Y. Liu, M.-H. Li, A. Zwaenepoel, H. Ma, B.
1910 Goffinet, Y.-L. Guan, J.-Y. Xue, Y.-Y. Liao, Q.-F. Wang, Q.-H. Wang, J.-Y. Wang, G.-Q.
1911 Zhang, Z.-W. Wang, Y. Jia, M.-Z. Wang, S.-S. Dong, J.-F. Yang, Y.-N. Jiao, Y.-L. Guo, H.-Z.
1912 Kong, A.-M. Lu, H.-M. Yang, S.-Z. Zhang, Y. Van de Peer, Z.-J. Liu, Z.-D. Chen, The
1913 hornwort genome and early land plant evolution, Nat Plants, 6 (2020) 107-118.
- 1914 [240] V. Ahmadjian, Trebouxia: Reflections on a Perplexing and Controversial Lichen
1915 Photobiont, in: J. Seckbach (Ed.) Symbiosis: Mechanisms and Model Systems, Springer
1916 Netherlands, Place Published, 2002, pp. 373-383.
- 1917 [241] L.R. Hoffman, Observations on the Fine Structure of *Oedogonium* IV. The Mature
1918 Pyrenoid of *Oe. cardiacum*, Trans. Am. Microsc. Soc., 87 (1968) 178-185.
- 1919 [242] S.P. Gibbs, The ultrastructure of the pyrenoids of green algae, J. Ultrastruct. Res., 7
1920 (1962) 262-272.
- 1921 [243] G.M. Lokhorst, H.J. Sluiman, W. Star, The Ultrastructure of Mitosis and Cytokinesis in
1922 the Sarcinoid *Chlorokybus atmophyticus* (Chlorophyta, Charophyceae) Revealed by Rapid
1923 Freeze Fixation and Freeze Substitution, J. Phycol., 24 (1988) 237-248.
- 1924 [244] S. Kikutani, K. Nakajima, C. Nagasato, Y. Tsuji, A. Miyatake, Y. Matsuda, Thylakoid
1925 luminal θ -carbonic anhydrase critical for growth and photosynthesis in the marine diatom
1926 *Phaeodactylum tricorutum*, Proc. Natl. Acad. Sci. U. S. A., 113 (2016) 9828-9833.
- 1927 [245] H.E. Calvert, C.J. Dawes, M.A. Borowitzka, Phylogenetic relationships of *Caulerpa*
1928 (Chlorophyta) based on comparative ultrastructure, J. Phycol., 12 (1976) 149-162.
- 1929 [246] J. Scott, E.-C. Yang, J.A. West, A. Yokoyama, H.-J. Kim, S.L. De Goer, C.J. O'Kelly, E.
1930 Orlova, S.-Y. Kim, J.-K. Park, Others, On the genus *Rhodella*, the emended orders
1931 Dixoniales and Rhodellales with a new order Glaucosphaerales (Rhodellophyceae,
1932 Rhodophyta), Algae, 26 (2011) 277-288.
- 1933 [247] T. Mikhailyuk, A. Lukešová, K. Glaser, A. Holzinger, S. Obwegeser, S. Nyporko, T.
1934 Friedl, U. Karsten, New Taxa of Streptophyte Algae (Streptophyta) from Terrestrial Habitats
1935 Revealed Using an Integrative Approach, Protist, 169 (2018) 406-431.
- 1936 [248] Y.D. Bedoshvili, T.P. Popkova, Y.V. Likhoshway, Chloroplast structure of diatoms of
1937 different classes, Cell tissue biol., 3 (2009) 297-310.

- 1938 [249] A. De Martino, A. Bartual, A. Willis, A. Meichenin, B. Villazán, U. Maheswari, C. Bowler,
 1939 Physiological and molecular evidence that environmental changes elicit morphological
 1940 interconversion in the model diatom *Phaeodactylum tricornutum*, *Protist*, 162 (2011) 462-
 1941 481.
- 1942 [250] K.L. McDonald, J.D. Pickett-Heaps, Ultrastructure and differentiation in *Cladophora*
 1943 *glomerata*. I. Cell division., *Am. J. Bot.*, 63 (1976) 592-601.
- 1944 [251] K.-I. Ishida, N. Ishida, Y. Hara, *Lotharella amoebiformis* sp. nov.: A new species of
 1945 chlorarachniophytes from Japan, *Phycological Res.*, 48 (2000) 221-229.
- 1946 [252] S.Y. Lee, H.J. Jeong, N.S. Kang, T.Y. Jang, S.H. Jang, T.C. Lajeunesse,
 1947 *Symbiodinium tridacnidorum* sp. nov., a dinoflagellate common to Indo-Pacific giant clams,
 1948 and a revised morphological description of *Symbiodinium microadriaticum* Freudenthal,
 1949 emended Trench & Blank, *Eur. J. Phycol.*, 50 (2015) 155-172.
- 1950 [253] J.D. Dodge, The Fine Structure of Chloroplasts and Pyrenoids in Some Marine
 1951 Dinoflagellates, *Journal of Cell Science*, 3 (1968) 41.
- 1952 [254] J. Deane, D. Hill, S. Brett, G. McFadden, *Hanusia phi* gen. et sp. nov. (Cryptophyceae):
 1953 characterization of 'Cryptomonas sp. Φ', *Eur. J. Phycol.*, 33 (1998) 149-154.
- 1954 [255] J. Fresnel, I. Probert, The ultrastructure and life cycle of the coastal coccolithophorid
 1955 *Ochrosphaera neapolitana* (Prymnesiophyceae), *Eur. J. Phycol.*, 40 (2005) 105-122.
- 1956 [256] S. Klöpffer, U. John, A. Zingone, O. Mangoni, W.H.C.F. Kooistra, A.D. Cembella,
 1957 Phylogeny and morphology of a *Chattonella* (Raphidophyceae) species from the
 1958 Mediterranean Sea: what is *C. subsalsa*?, *Eur. J. Phycol.*, 48 (2013) 79-92.
- 1959 [257] J.L. Scott, B. Baca, F.D. Ott, J.A. West, Light and Electron Microscopic Observations
 1960 on *Erythrolobus coxiae* gen. et sp. nov. (Porphyridiophyceae, Rhodophyta) from Texas USA,
 1961 *Algae*, 21 (2006) 407-416.
- 1962 [258] F. Jouenne, W. Eikrem, F. Le Gall, D. Marie, G. Johnsen, D. Vaultot, *Prasinoderma*
 1963 *singularis* sp. nov. (Prasinophyceae, Chlorophyta), a solitary coccoid Prasinophyte from the
 1964 South-East Pacific Ocean, *Protist*, 162 (2011) 70-84.
- 1965 [259] J.D. Dodge, The fine structure of chloroplasts and pyrenoids in some marine
 1966 dinoflagellates, *J. Cell Sci.*, 3 (1968) 41-47.
- 1967 [260] S. Flori, P.-H. Jouneau, G. Finazzi, E. Maréchal, D. Falconet, Ultrastructure of the
 1968 Periplastidial Compartment of the Diatom *Phaeodactylum tricornutum*, *Protist*, 167 (2016)
 1969 254-267.
- 1970 [261] T. Hori, Comparative Studies of Pyrenoid Ultrastructure in algae of the *Monostroma*
 1971 *Complex*, *J. Phycol.*, 9 (1973) 190-199.
- 1972 [262] J.D. Dodge, The Fine Structure of Algal Cells, Academic Press, Place Published, 1973.
- 1973 [263] E. Kusel-Fetzmann, M. Weidinger, Ultrastructure of five *Euglena* species positioned in
 1974 the subdivision Serpentes, *Protoplasma*, 233 (2008) 209-222.
- 1975 [264] M.E. Bakker, G.M. Lokhorst, Ultrastructure of mitosis and cytokinesis in *Zygnema* sp.
 1976 (Zygnematales, Chlorophyta), *Protoplasma*, 138 (1987) 105-118.
- 1977 [265] T. Zhan, W. Lv, Y. Deng, Multilayer gyroid cubic membrane organization in green alga
 1978 *Zygnema*, *Protoplasma*, 254 (2017) 1923-1930.
- 1979 [266] K. Trumhová, A. Holzinger, S. Obwegeser, G. Neuner, M. Pichrtová, The conjugating
 1980 green alga *Zygnema* sp. (Zygnematophyceae) from the Arctic shows high frost tolerance in
 1981 mature cells (pre-akinetes), *Protoplasma*, 256 (2019) 1681-1694.
- 1982 [267] L. Van Thinh, D.J. Griffiths, H. Winsor, Ultrastructure of *Symbiodinium microadriaticum*
 1983 (Dinophyceae) symbiotic with *Zoanthus* sp. (Zoanthidea), *Phycologia*, 25 (1986) 178-184.
- 1984 [268] M. Oborník, M. Vancová, D.-H. Lai, J. Janouškovec, P.J. Keeling, J. Lukeš,
 1985 Morphology and ultrastructure of multiple life cycle stages of the photosynthetic relative of
 1986 apicomplexa, *Chromera velia*, *Protist*, 162 (2011) 115-130.
- 1987 [269] G. Gärtner, B. Uzunov, E. Ingolic, W. Kofler, G. Gacheva, P. Pilarski, L. Zagorchev, M.
 1988 Odjakova, M. Stoyneva, Microscopic investigations (LM, TEM and SEM) and identification of
 1989 *Chlorella* isolate R-06/2 from extreme habitat in Bulgaria with a strong biological activity and
 1990 resistance to environmental stress factors, *Biotechnol. Biotechnol. Equip.*, 29 (2015) 536-
 1991 540.

1992 [270] T. Mikhailyuk, A. Holzinger, A. Massalski, U. Karsten, Morphology and ultrastructure of
1993 Interfilum and *Klebsormidium* (Klebsormidiales, Streptophyta) with special reference to cell
1994 division and thallus formation, *Eur. J. Phycol.*, 49 (2014) 395-412.

1995 [271] E.A. Ainsworth, S.P. Long, What have we learned from 15 years of free-air CO₂
1996 enrichment (FACE)? A meta-analytic review of the responses of photosynthesis, canopy
1997 properties and plant production to rising CO₂, *New Phytol.*, 165 (2005) 351-372.

1998 [272] X.-G. Zhu, S.P. Long, D.R. Ort, What is the maximum efficiency with which
1999 photosynthesis can convert solar energy into biomass?, *Curr. Opin. Biotechnol.*, 19 (2008)
2000 153-159.

2001 [273] L.C.M. Mackinder, The *Chlamydomonas* CO₂-concentrating mechanism and its
2002 potential for engineering photosynthesis in plants, *New Phytol.*, 217 (2018) 54-61.

2003 [274] B.D. Rae, B.M. Long, B. Förster, N.D. Nguyen, C.N. Velanis, N. Atkinson, W.Y. Hee, B.
2004 Mukherjee, G.D. Price, A.J. McCormick, Progress and challenges of engineering a
2005 biophysical carbon dioxide-concentrating mechanism into higher plants, *J. Exp. Bot.*, 68
2006 (2017) 3717-3737.

2007 [275] M.T. Meyer, A.J. McCormick, H. Griffiths, Will an algal CO₂-concentrating mechanism
2008 work in higher plants?, *Curr. Opin. Plant Biol.*, 31 (2016) 181-188.

2009 [276] J.M. McGrath, S.P. Long, Can the Cyanobacterial Carbon-Concentrating Mechanism
2010 Increase Photosynthesis in Crop Species? A Theoretical Analysis, *Plant Physiology*, 164
2011 (2014) 2247.

2012 [277] A. Wu, G.L. Hammer, A. Doherty, S. von Caemmerer, G.D. Farquhar, Quantifying
2013 impacts of enhancing photosynthesis on crop yield, *Nature Plants*, 5 (2019) 380-388.

2014 [278] P.F. South, A.P. Cavanagh, H.W. Liu, D.R. Ort, Synthetic glycolate metabolism
2015 pathways stimulate crop growth and productivity in the field, *Science*, 363 (2019) eaat9077.

2016 [279] J. Kromdijk, K. Głowacka, L. Leonelli, S.T. Gabilly, M. Iwai, K.K. Niyogi, S.P. Long,
2017 Improving photosynthesis and crop productivity by accelerating recovery from
2018 photoprotection, *Science*, 354 (2016) 857.

2019 [280] P.E. López-Calcano, K.L. Brown, A.J. Simkin, S.J. Fisk, S. Violet-Chabrand, T.
2020 Lawson, C.A. Raines, Stimulating photosynthetic processes increases productivity and
2021 water-use efficiency in the field, *Nature Plants*, 6 (2020) 1054-1063.

2022 [281] N. Atkinson, D. Feike, L.C.M. Mackinder, M.T. Meyer, H. Griffiths, M.C. Jonikas, A.M.
2023 Smith, A.J. McCormick, Introducing an algal carbon-concentrating mechanism into higher
2024 plants: location and incorporation of key components, *Plant Biotechnol. J.*, 14 (2016) 1302–
2025 1315.

2026 [282] N. Atkinson, N. Leitão, D.J. Orr, M.T. Meyer, E. Carmo-Silva, H. Griffiths, A.M. Smith,
2027 A.J. McCormick, Rubisco small subunits from the unicellular green alga *Chlamydomonas*
2028 complement Rubisco-deficient mutants of *Arabidopsis*, *New Phytol.*, 214 (2017) 655-667.

2029 [283] N. Atkinson, Y. Mao, K.X. Chan, A.J. McCormick, Condensation of Rubisco into a
2030 proto-pyrenoid in higher plant chloroplasts, *Nature Communications*, 11 (2020) 6303.

2031 [284] B.M. Long, W.Y. Hee, R.E. Sharwood, B.D. Rae, S. Kaines, Y.-L. Lim, N.D. Nguyen, B.
2032 Massey, S. Bala, S. von Caemmerer, M.R. Badger, G.D. Price, Carboxysome encapsulation
2033 of the CO₂-fixing enzyme Rubisco in tobacco chloroplasts, *Nat. Commun.*, 9 (2018) 3570.
2034